

DISSERTATION

Systematic search for microRNA regulated target genes with roles in the
etiology of periodontitis

Systematische Suche nach mikroRNA-regulierten Zielgenen mit Rolle in
der Ätiologie der Parodontitis

zur Erlangung des akademischen Grades
Doctor medicinae dentariae (Dr. med. dent.)

vorgelegt der Medizinischen Fakultät
Charité – Universitätsmedizin Berlin

von
Luyang Zheng

Erstbetreuung: Univ.-Prof. Dr. rer. nat. Arne Schäfer

Datum der Promotion: 23.03.2024

Contents

List of Tables.....	v
List of Figures	vi
Abbreviations	vii
Zusammenfassung.....	1
Abstract	3
1 Introduction	4
2 Materials and Methods	8
2.1 Materials.....	8
2.1.1 Kits, chemicals and solutions	8
2.1.2 Enzymes and buffers	9
2.1.3 miRNA mimics	10
2.1.4 Consumables	11
2.1.5 Devices	11
2.1.6 Antibodies	12
2.1.7 Plasmid and cell line	13
2.1.8 Oligonucleotides.....	13
2.1.9 Media and buffers.....	14
2.1.10 Software tools and websites	15
2.2 Methods.....	16
2.2.1 miRNA selection	16
2.2.2 Isolation and Cultivation of Primary Human Gingival Fibroblasts (phGFs)	18
2.2.3 miRNA transfection	19
2.2.4 Total RNA extraction	19
2.2.5 RNA sequencing (RNA-seq).....	20
2.2.6 qRT-PCR.....	20

2.2.6.1 RNA purification.....	20
2.2.6.2 cDNA synthesis.....	21
2.2.6.3 qRT-PCR primer design.....	21
2.2.6.4 qRT-PCR.....	22
2.2.7 Cloning of <i>CPEB1</i> 3'UTR sequence into the reporter plasmid pGL4.24.....	23
2.2.7.1 Polymerase chain reaction (PCR)	23
2.2.7.2 Restriction digest.....	23
2.2.7.3 Gel electrophoresis	24
2.2.8 Purification of DNA fragments	24
2.2.9 Ligation	25
2.2.10 Transformation	25
2.2.11 Plasmid DNA isolation.....	26
2.2.12 DNA sequencing	26
2.2.13 Co-transfection of plasmid DNA and miRNAs	27
2.2.13.1 Cultivation of ihGFs for reporter gene assays and Western Blotting	27
2.2.13.2 Transfection of ihGFs with dual reporter gene plasmids	27
2.2.14 Luciferase Reporter gene assays	28
2.2.15 Quantitative reverse transcription polymerase chain reaction (qRT-PCR).....	28
2.2.16 Protein expression analysis	29
2.2.16.1 Protein extraction	29
2.2.16.2 Protein concentration measurement	30
2.2.17 Western Blotting	30
2.2.17.1 Protein Sample Preparation	30
2.2.17.2 SDS-PAGE.....	30
2.2.17.3 Protein transfer	31
2.2.17.4 Immunoblotting.....	32
3. Results	33

3.1 Contrast results for differentially expressed miRNAs find periodontitis risk genes as miRNA target genes.....	33
3.2 Validation of the inhibitory effect of hsa-miR-130a-3p on the 3'UTR sequence of <i>CPEB1</i>	40
3.3 Validation of the effect of hsa-miR-130a-3p on protein expression through dual luciferase reporter gene assay	40
3.4 All miRNAs significantly upregulated the gene <i>MET</i>	41
3.5 Validation of the upregulation effect of hsa-miR-17-5p, -30e-5p, -223-3p, -142-3p, -130a-3p, -144-3p, -144-5p on the gene <i>MET</i> via Western blotting.	43
3.6 Gene set enrichment analyses	44
4. Discussion	50
5. Conclusion.....	53
References	54
Statutory Declaration.....	58
Curriculum Vitae.....	59
Acknowledgements.....	60
Confirmation by a statistician	61

List of Tables

Table 1: Kits, chemicals and solutions	7
Table 2: Enzymes and buffers	8
Table 3: miRNA mimics	9
Table 4: Consumables	10
Table 5: Devices.....	10
Table 6: Antibodies.....	13
Table 7: Plasmid and cell line.....	13
Table 8.1: Oligonucleotides	13
Table 8.2: Oligonucleotides used for qRT-PCR	13
Table 9: Media and Buffers	14
Table 10: Software tools and websites	15
Table 11: Differentially expressed miRNAs in healthy and inflamed gingival biopsies found in the indicated miRNA array-based studies.....	17
Table 12: PCR program of cDNA synthesis	20
Table 13: qRT-PCR program.	22
Table 14: PCR program for 3'UTR of <i>CPEB 1</i>	23
Table 15: Standard curve measurement.	30
Table 16: SDS page preparation chemicals.....	30
Table 17: The order of the transfer sandwich.....	31
Table 18: The 10 most downregulated genes after miRNA transfection into phGFs.....	37
Table 19: Genes that were upregulated by ≥ 3 miRNAs.....	41
Table 20: The most significantly enriched gene set for each gene set collection after miRNA transfection into phGFs.....	47

List of Figures

Figure 1. Schematic of healthy tooth side and periodontitis side.....	5
Figure 2. Model of miRNA regulation.....	6
Figure 3. Workflow of the study.....	16
Figure 4. 1% agarose gel picture of restricted PCR product of CPEB1 3' UTR on the left and restricted pGL4.24 vector on the right.....	23
Figure 5. Sequence alignment of <i>CPEB1</i> -3'UTR.....	26
Figure 6. 1% agarose gel picture of PCR to check genomic DNA contamination of cDNA.....	28
Figure 7. A-G. Volcano plots for differentially regulated genes after miRNA transfection into phGFs.....	34
Figure 8. miR-130a-3p downregulates <i>CPEB1</i> -3'UTR Luc reporter gene expression in ih-GFs.....	39
Figure 9. miR-130a-3p downregulates <i>CPEB1</i> -3'UTR Luc protein activity in ihGFs....	40
Figure 10. A-D. qRT-PCR of gene <i>MET</i> , <i>RBPJ</i> , <i>DDX3Y</i> and <i>SLC36A1</i> expression on transfected phGFs.....	41
Figure 11. Western blot showed that all of the miRNAs obviously upregulate protein <i>MET</i> expression in ihGFs.....	43
Figure 12. Evidence plots of enriched gene sets indicated cell cycle and innate immunity pathways as being regulated by each of the miRNAs.....	45

Abbreviations

Amp.	Amplicilin
APS	Ammonium persulfate
ATP	Adenosine triphosphate
ATP6V1C1	ATPase H ⁺ Transporting V1 Subunit C1
ABCA1	ATP Binding Cassette Subfamily A Member 1
AUC	Area under curve
Bp	Basepairs
BSA	Bovine serum albumin
cDNA	Complementary DNA
cm	Centimeter
CPEB1	Cytoplasmic Polyadenylation Element Binding Protein 1
DNA	Deoxyribonucleic acid
dNTPs	Deoxyribonucleoside triphosphate
DPBS	Dulbecco's phosphate-buffered saline
DMEM	Dulbecco's Modified Eagle Medium
ECM	Extracellular matrix
EDTA	Ethylenediaminetetraacetic acid
e.g.	Exempli gratia (for example)
EtOH	Ethanol
EtBr	Ethidium bromide
FBS	Fetal bovine serum
FC	Fold change
Fw	Forward

G	Gram
GAPDH	Glyceraldehyde-3-phosphate dehydrogenase
GO	Gene Ontology
h	Hours
HRP	Horseradish peroxidase
Kb	Kilobases
Kda	1,000 daltons
LPS	lipopolysaccharide
mA	milli ampere
mg	Milligram
MET	MET Proto-Oncogene, Receptor Tyrosine Kinase
MeTH	Methanol
um	Micrometer
miRNA	microRNA
min	Minutes
mL	Milliliters
mM	Millimolar
mRNA	messenger RNA
NaCl	sodium chloride
NaOH	sodium hydroxide
NEAA	non-essential amino acids
Ng	Nanogram
Nm	Nanometer
Nt	Nucleotides
Padj	adjusted P-value
PCR	polymerase chain reaction

PD	Periodontitis
pGF	primary gingival fibroblast cells
pmol	Picomole
PTK9	Protein Tyrosine Kinase 9
qRT-PCR	quantitative reverse transcriptase polymerase chain reaction
PCR	Polymerase chain reaction
RNA	ribonucleic acid
RPM	rounds per minute
Rev	Reverse
RT	room temperature
SDS	sodium dodecyl sulfate
Sec	Seconds
Tris	Tris(hydroxymethyl) aminomethane
TEMED	Tetramethylethylenediamine
U	Units
UPW	ultrapure water (RNase- and DNase-free)
V	Volt
YT-medium	medium with yeast extract and tryptone

Zusammenfassung

Ziele. Mehrere arraybasierte miRNA-Expressionsstudien haben unabhängig voneinander eine erhöhte Expression der miRNA hsa-mir-130a-3p, -142-3p, -144-3p, -144-5p, -223-3p, -17-5p und -30e-5p im entzündeten Zahnfleisch von Patienten mit Parodontitis im Vergleich zu gesunden Kontrollen gezeigt. Unser Ziel war es, direkte Zielgene und Signalwege zu bestimmen, die durch diese miRNAs reguliert werden.

Material und Methoden. Wir transfizierten einen miRNA-Mimetikum (mirVana) jeder miRNA in Kulturen humaner primärer Zahnfleischfibroblasten, die aus dem Zahnfleisch von drei verschiedenen Spendern isoliert wurden. Nach RNA-Sequenzierung wurde die differentielle Genexpression mit DESeq2 analysiert. Die Analyse der Anreicherung verschiedener Gen-Sets erfolgte mit MSigDB, den tmod- und goseq-Paketen. Die Hemmung und Hochregulierung der miRNAs wurden auf der Transkript- und Proteinebene mit quantitativer RT-PCR, Western-Blotting und Reporter-Gen Assays validiert.

Ergebnisse. Die Gen-Set-Anreicherung zeigte signifikante Rollen für die Regulation des Zellzyklus von hsa-miR-130a-3p ($P_{adj}=5\times10^{-15}$), miRNA-144-3p und -5p ($P_{adj}=4\times10^{-40}$ und $P_{adj}=4\times10^{-6}$), miR-17-5p ($P_{adj}=9.5\times10^{-23}$) und miR-30e-5p ($P_{adj}=8.2\times10^{-18}$). Darüber hinaus wurden signifikante Rollen in der Zytokinsignalgebung für miR-130a-3p ($P_{adj}=5\times10^{-15}$), miR-223-3p ($P_{adj}=2.4\times10^{-7}$) und miR-142-3p ($P_{adj}=5\times10^{-11}$) gezeigt. Die Gene *WASL*, *ENPP5*, *MANBAL*, *IDH1* zeigten die signifikanteste und stärkste Inhibition nach der Transfektion von hsa-miR-142-3p, -17-5p, -223-3p und -30e-5p, respektive. Darüber hinaus regulierten hsa-miR-130a-3p, -144-3p und -144-5p die Parodontitisrisikogene *CPEB1*, *ABCA1* und *ATP6V1C1*. In unserer Studie zeigte die Expression aller analysierten miRNAs eine signifikante positive Korrelation mit der Expression des Gens *MET*, das an der Wundheilung sowie an der Geweberegeneration und -umgestaltung beteiligt ist.

Schlussfolgerung. Die differentielle Expression von Gen-Sets der Zytokinsignalgebung und der Regulation der Zellproliferation nach Überexpression der untersuchten miRNAs weist auf ihre Bedeutung für die Ätiologie der Parodontitis hin. Darüber hinaus liefert die Identifikation der Parodontitisrisikogene *CPEB1*, *ABCA1* und *ATP6V1C1* als Zielgene einiger der untersuchten miRNAs weitere Hinweise für ihre Bedeutung in der Ätiologie der Parodontitis. Gingivale miRNAs führen komplexe regulatorische Netzwerke derart zusammen, dass sie zu einer verstärkten Expression des Gens *MET* führen. Dies betont die Bedeutung von *MET*, einem

Rezeptor des fibroblastensezernierten mitogenen Hepatozytenwachstumsfaktors, für das Krankheitsgeschehen im Anschluß an die aktive orale Entzündung.

Abstract

Aims. Several array-based miRNA expression studies indicated increased transcript levels of hsa-miR-130a-3p, -142-3p, -144-3p, -144-5p, -223-3p, -17-5p and -30e-5p in the inflamed gingiva of periodontitis patients compared to healthy controls. We aimed to determine direct target genes and signaling pathways that are regulated by these miRNAs.

Material and Methods. We transfected a miRNA mimic (mirVana) of each miRNA into human primary gingival fibroblasts cultured from 3 different donors. Following RNA-Sequencing, differential gene expression was analysed using DESeq2. Gene set enrichment analysis was performed with MSigDB, and the tmod and goseq packages. miRNA inhibition and upregulation were validated for selected genes on the transcript and protein level using quantitative RT-PCR, Western blotting and reporter gene assays.

Results. Gene set enrichment demonstrated significant roles for cell cycle regulation of hsa-miR-130a-3p ($P_{adj}=5\times10^{-15}$), miRNA-144-3p and -5p ($P_{adj}=4\times10^{-40}$ and $P_{adj}=4\times10^{-6}$), miR-17-5p ($P_{adj}=9.5\times10^{-23}$) and miR-30e-5p ($P_{adj}=8.2\times10^{-18}$). Additionally, significant roles in cytokine signaling were shown for miR-130a-3p ($P_{adj}=5\times10^{-15}$), miR-223-3p ($P_{adj}=2.4\times10^{-7}$) and miR-142-3p ($P_{adj}=5\times10^{-11}$). The genes *WASL*, *ENPP5*, *MANBAL*, *IDH1* showed the most significant and strongest downregulation after hsa-miR-142-3p, -17-5p, -223-3p and -30e-5p transfection, respectively. Moreover, hsa-miR-130a-3p, -144-3p and -144-5p regulated the periodontitis risk genes *CPEB1*, *ABCA1* and *ATP6V1C1*, respectively. Furthermore, we found that all analyzed miRNAs significantly increased the expression of the gene *MET*, which participates in wound healing as well as tissue regeneration and remodeling.

Conclusion. Gene set enrichment emphasized the significance of cytokine signaling and the regulation of cell proliferation in the etiology of periodontitis and adds evidence for *CPEB1*, *ABCA1* and *ATP6V1C1* as susceptibility genes of periodontitis. *MET* may play an important role in the etiology of periodontitis.

Key Words. miRNA; *MET*; cell cycle; mesenchymal cellular migration; periodontitis; *CPEB1*; *ABCA1*; *ATP6V1C1*

1 Introduction

Periodontitis (PD) is a common disease of the periodontal tissue and a leading cause of tooth loss ((Eke et al. 2012); (Nesse et al. 2008)). It is the main cause of tooth loss in adults and affects about 11 % of the world population (Vos et al. 2012), impairing the health and life quality of a substantial share of the population and causing high costs for public health systems. Its main symptoms include inflammation of the oral mucosa and supporting tissues - which can cause bleeding gums, formation of periodontal pockets and loss of connective tissue and alveolar bone, followed by tooth loss (**Figure 1**). A significant risk factor for PD is long-term gingivitis, characterized by swelling and bleeding gums.

Current research indicates that the etiology of periodontitis is complex (Meyle and Chapple 2015), involving the interaction of multiple factors. The most significant factor is widely recognized as dental plaque (Lang et al. 2009), a sticky substance formed by bacteria in the oral cavity that can trigger gingivitis and periodontitis. Other factors include genetic factors (Loos et al. 2005), oral hygiene habits (Bakdash 1994), smoking (Hamdi et al. 2021), dietary habits (Altun et al. 2021), hormonal changes (Mascarenhas et al. 2003), diabetes (Preshaw and Bisset 2019), and medication use (Heasman and Hughes 2014). These factors may lead to changes in the type and quantity of bacteria in the oral cavity, resulting in damage to periodontal tissues and the occurrence of inflammatory responses. However, since the patient's immune system varies over time and may be impacted by lifestyle choices, other illnesses, or age, the individual genetic composition may also change with time, for example via epigenetic impacts or somatic mutations. As a consequence, periodontitis is perceived to be a complex disease (Nield 2021). In the complex interplay between intrinsic and extrinsic factors, including the immune system, oral infections, and the consequences of lifestyle choices, genes play a key role. Therefore, an improved understanding of the molecular mechanisms of periodontitis that drive disease pathogenesis would improve prevention and treatment options in the future.

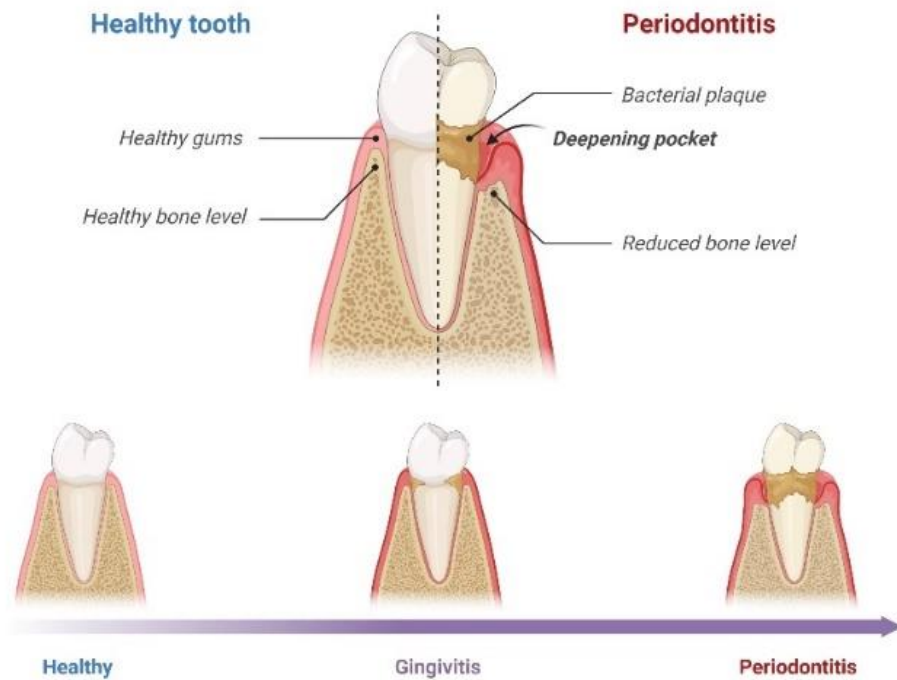


Figure 1. Schematic of healthy tooth side and periodontitis side. The image displays healthy gingival tissue and alveolar bone on the left, while on the right, there is periodontal tissue inflammation and alveolar bone destruction, often resulting from the presence of a pathogenic dysbiotic biofilm (PD). The bottom figure illustrates the progression of periodontal tissue from a healthy state to periodontitis (modified on BioRender; <https://www.biorender.com/>).

MicroRNAs (miRNAs) are short single-stranded, non-protein coding RNAs with inhibiting functions on gene activity, generally by interacting with the 3'-untranslated regions (3'UTR) of target protein coding messenger RNAs (mRNAs) (Ha and Kim 2014). Individual miRNAs modulate the expression of distinct genes and, thereby, can affect complex gene networks (Selbach et al. 2008). As a result, miRNAs modulate a range of biological processes. Likewise, miRNAs are involved in complex diseases and affected tissues show differential miRNA expression (Paul et al. 2018). To identify miRNAs that are differentially expressed in periodontitis, various studies generated array-based expression profiles of miRNAs in healthy and inflamed periodontal tissues and reported differential expression of numerous miRNAs in the gingiva (Lee et al. 2011; Ogata et al. 2014; Perri et al. 2012; Stoecklin-Wasmer et al. 2012; Xie et al. 2011) and saliva (Fujimori et al. 2019). However, the target genes and biological processes that are regulated by these miRNAs in periodontal tissues have remained unknown.

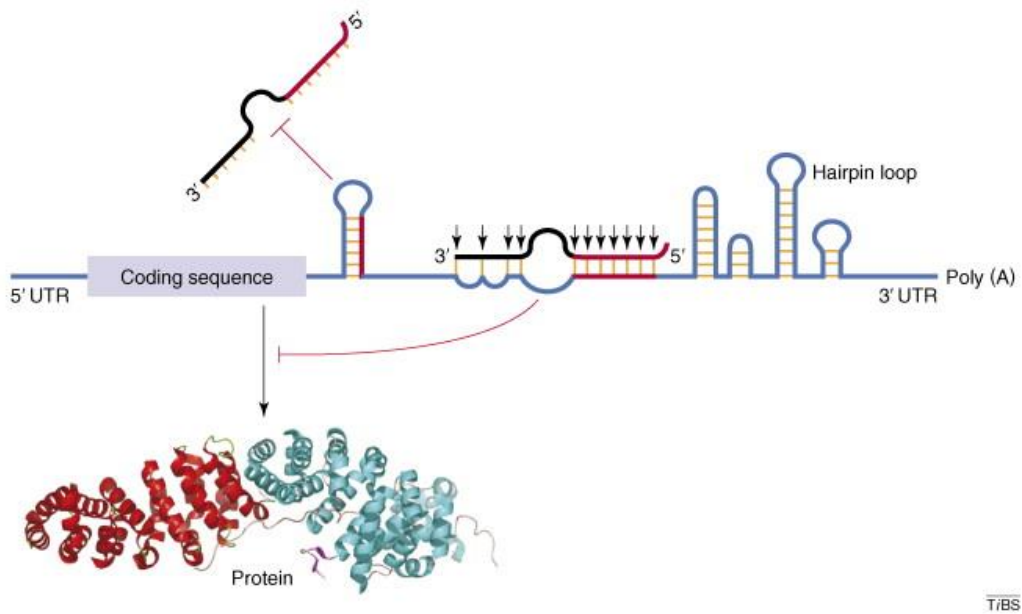


Figure 2. Model of miRNA regulation (taken from Zhao and Srivastava 2007). The miRNA binds to the 3'UTR at a specific recognition site (hairpin), which leads to conformational changes that affect transcription or translation by changes in mRNA stability or translation initiation.

I hypothesized that differently expressed miRNAs are suitable targets for the identification of genes and functional gene networks which are directly involved in the etiology of periodontitis. This is because overall, miRNAs are predicted to target only ~10–30% of protein-coding genes, with each miRNA repressing on average 200 transcripts (Brennecke et al. 2005; Lall et al. 2006; Lewis et al. 2005). This considerably reduces the level of complexity and can be a straightforward approach to identify genes and pathways with relevant functions in disease development and restoring health. In the current study, we hypothesized that genes and gene networks that are directly regulated by miRNAs upregulated in inflamed periodontal tissues would reveal mechanisms with relevant functions for the disease etiology. However, a limitation of studying biological processes in gingival biopsies is that they consist of multiple different tissue types and, in particular, inflamed gingival samples have a share of up to 50% of invaded immune cells (Richter et al. 2021). Moreover, variation in the ratio of different cell types can be caused by different sampling times and differences in the analysis design between studies also can influence results. Therefore, individual observations by single studies have to be interpreted with caution. In contrast, differentially expressed genes found independently by several studies that aimed to investigate the same disease state are more likely to be truly involved. Therefore, I selected miRNAs that several miRNA expression profiling studies independently showed to be higher expressed in gingival biopsies collected immediately prior to periodontal surgery and which therefore can be considered as non-

actively inflamed. I overexpressed these miRNAs in human primary gingival fibroblasts and performed genomewide expression profiling to identify miRNA regulated genes and gene sets.

Aims of the study

- Identification of candidate miRNAs that showed upregulation in several previous miRNA array-based studies performed with inflammation affected and healthy gingival tissues.
- Identification of genes and gene sets that are regulated in response to increased expression of the selected candidate miRNAs in gingival fibroblasts.
- *In vitro* validation of selected genes that showed regulation by these miRNAs.

2 Materials and Methods

2.1 Materials

2.1.1 Kits, chemicals and solutions

Table 1: Kits, chemicals and solutions

Kits, chemicals, solutions	Manufacturer
Acrylamide-solution (30%)	SERVA Electrophoresis
Agar	AppliChem
Agarose	SERVA Electrophoresis
Ampicillin	Gibco by life technologies
Ammonium Persulfate (APS)	Amresco
β -mercaptoethanol	Carl Roth
Bacto Tryptone	BD Bacto
Bacto Yeast Extract	BD Bacto
BCA protein assay	Thermo Fisher Scientific
Bovine serum albumin (BSA)	SERVA Electrophoresis
Dulbecco's Modified Eagle Medium (DMEM)	PAN Biotech
Deoxynucleotides (dNTPs) Mix (100 mM)	Thermo Fisher Scientific
Dulbecco's phosphate-buffered saline (DPBS)	Gibco by life technologies
Dual Luciferase Reporter Assay	Promega
Ethanol (70%, dehydrated)	Carl Roth
Ethanol (99.9%)	Merck
Ethidium bromide (EtBr)	Carl Roth
Ethylenediaminetetraacetic acid (EDTA)	Sigma-Aldrich
ECL Western Blotting Substrate	Thermo Fisher Scientific
Fetal Bovine Serum (FBS)	Gibco by life technologies
GeneRuler 1 kb DNA Marker	Thermo Fisher Scientific
Glycerol	Carl Roth
Gibson Assembly Cloning Kit	New England Biolabs
High-Capacity cDNA Reverse Transcription Kit	Applied Biosystems

Isopropanol	Sigma Aldrich
Lipofectamine RNAiMax	Thermo Fisher Scientific
Lipofectamine 2000	Thermo Fisher Scientific
Loading Dye 6x	Thermo Fisher Scientific
Nuclear Protein extraction Kit	Active Motif
Opti-Mem Reduced Serum Medium	Life Technologies
Oligo dTs	Thermo Fisher Scientific
O'Range Ruler 50 bp Ladder	Thermo Fisher Scientific
Prestained Protein Ladder, 10 to 180 kDa	Thermo Fisher Scientific
QIAprep Spin Miniprep Kit	Qiagen
Qiagen Plasmid Midi Kit	Qiagen
QIAprep Spin Miniprep Kit	Qiagen
QIAquick Gel Extraction Kit	Qiagen
RNeasy Mini Kit	Qiagen
SOC Medium	Invitrogen
Sodium acetate 3M	Sigma-Aldrich
Sodium chloride 150 mM	Polyplus-transfection
SYBR Select Master Mix	Thermo Fisher Scientific
Tetramethylethylenediamine (TEMED)	Sigma-Aldrich
Tris(hydroxymethyl)aminomethane (Tris)	Sigma-Aldrich
Trypsin/EDTA	PAN Biotech
Ultrapure Water	Qiagen

2.1.2 Enzymes and buffers

Table 2: Enzymes and buffers

Enzymes and buffers	Manufacturer
Alkaline Phosphatase, Calf Intestinal (CIP), 10,000 U/mL	New England Biolabs
rCut Smart Buffer	New England Biolabs
DNase I recombinant, 10 U/µL	Roche

FseI, 2,000 units/ml	New England Biolabs
HF Buffer	Thermo Fisher Scientific
MultiScribe Reverse Transcriptase, 50 U/ μ L	Invitrogen
Phusion High-Fidelity Polymerase 2 U/ μ L	Thermo Fisher Scientific
Reaction Buffer 10 x	Biozym
RT-Buffer 10 x	Invitrogen
RNaseOut Recombinant Ribonuclease Inhibitor, 40 U/ μ L	Invitrogen
Taq DNA Polymerase, 5 U/ μ L	Biozym
T4 Ligase	New England Biolabs
T4 Ligase Buffer	New England Biolabs
T4 Polynucleotide Kinase	New England Biolabs
50x TAE Buffer	Rotiphorese
XbaI, 20,000 U/mL	New England Biolabs

2.1.3 miRNA mimics

Table 3: miRNA mimics

miRNA mimics	Manufacturer
mirVana miR-130a-3p	Thermo Fisher Scientific
mirVana miR-142-3p	Thermo Fisher Scientific
mirVana miR-144-3p	Thermo Fisher Scientific
mirVana miR-144-5p	Thermo Fisher Scientific
mirVana miR-30e-5p	Thermo Fisher Scientific
mirVana miR-17-5p	Thermo Fisher Scientific
mirVana miR-223-3p	Thermo Fisher Scientific
mirVana miR-1 Positive Control	Thermo Fisher Scientific
mirVana miRNA Inhibitor, Negative Control #1	Thermo Fisher Scientific

2.1.4 Consumables

Table 4: Consumables

Consumables	Manufacturer
1.5 mL and 2 mL microcentrifuge tubes	Eppendorf
6-Well plate (sterile)	Techno Plastic Products (TPP)
Biosphere Filtertips (10 µL, 20 µL, 100 µL, 200 µL, 1000 µL)	Sarstedt
Cell culture flasks (T75-T300)	TPP
Cell scraper (24 cm)	Sarstedt
Falcon tips (5mL, 10mL, 25mL)	Falcon
Falcon tubes (15 mL, 50 mL)	Falcon
Filter paper (extra thick blot paper)	Bio-Rad
Multiplate 96-well white PCR plates	Bio-Rad
PCR strips and reaction tubes	Carl Roth
Petri dishes (plastic)	Sarstedt
PVDF membrane	Bio-Rad
Syringe (1mL, 5mL)	Braun

2.1.5 Devices

Table 5: Devices

Devices	Manufacturer
Battery-operated pipette controller	Brand
Benchtop centrifuge	Thermo Fisher Scientific/Heraeus
CFX Connect Real-Time PCR Detection System	Bio-Rad

Chemiluminescence Imager ChemoStar Touch	Intas
Electrophoresis chamber for agarose gels	Biometra
Electrophoresis chamber	Bio-Rad
Freezer -80°C MDF-U72V	SANYO
Freezer -20 °C	Liebherr
Incubator for cell culture	Heraeus Instruments
Light microscope	Leitz
Liquid nitrogen tank Arpege 40	Air Liquide
Microwave	Bosch
Multiskan GO Spectrophotometer	Thermo Fisher Scientific
Orion II Microplate Luminometer	Berthold
PCR FlexCycler	Analytik Jena
pH-Meter 766 Calimatic	Knick
Shaking incubator for bacterial culture	VWR
Sterile bench	Thermo Fisher Scientific
Standard power pack p25T	Analytik Jena
UV transparent gel trays	Biometra
Vortex Genie 2	Scientific Industries
Waterbath for cell culture	Julabo MWB
Weight machine	Analytical Plus
Western blotting system	Bio-Rad

2.1.6 Antibodies

Table 6: Antibodies

Antibodies	Manufacturer
β-actin(C4)	Santa Cruz Biotechnology
Met (25H2) Mouse mAb	Cell Signaling Technology
CPEB1 (ab3465)	Abcam
Anti-Mouse IgG, HRP (7076)	Cell Signaling Technology
Anti-Rabbit IgG, HRP (A16172)	Invitrogen

2.1.7 Plasmid and cell line

Table 7: Plasmid and cell line

Plasmid / cell line	Manufacturer
Plasmid: pGL4.24	Promega
Cell: Immortalized Human Gingival Fibroblast	ABM

2.1.8 Oligonucleotides

Table 8.1: Oligonucleotides

Gene	Forward (5'-3')	Reverse (5'-3')
<i>CPEB1</i>	ATT TCT AGA GGC AGG TCA GGC AAG CAG	GGA CCG GCC GGC CCC ACC GAA AAG CAG CCC T

Table 8.2: Oligonucleotides used for qRT -PCR

Gene	Forward (5'-3')	Reverse (5'-3')
<i>MET</i>	CCC GAA GTG TAA GCC CAA CT	TGC ACA ATC AGG CTA CTG GG
<i>RBPJ</i>	CAC TCC TGT GCC TGT GGT AG	CGG ACC CAT CTC CAA CCT TC

<i>DDX3Y</i>	GGA CGT GTA GGA AAC CTG GG	GGC ACC AAA TCC TCC ACT GA
<i>SLC36A1</i>	GCT GGG ATT CTG CTG TGT CT	TGG CAG TTA TTG GTG GTC CC
<i>GAPDH</i>	CAA ATT CCA TGG CAC CGT CA	CCT GCA AAT GAG CCC CAG
<i>PTK9</i>	AGC TCA ACT ATG TGC AGT TGG AAA	ACG AGC TGA ATC CTT GGG AA
<i>Luc (Luciferase)</i>	ACG TGC AAA AGA AGC TAC CG	GGC AAA TGG GAA GTC AGA A
<i>pGL4.24 Backbone</i>	TTC AAC CCA GTC AGC TCC TT	CAA GAA CTC TGT AGC ACC GC

2.1.9 Media and buffers

Table 9: Media and buffers

Media and buffers	Components
YT medium (1L)	(1)16 g Tryptone (2)10 g Yeast extract (3)5 g NaCl (4)15 g Agar (5)Add ddH ₂ O, adjust volume to 1 L(pH 7.0)
10X Transfer buffer (1L)	(1) 30.3g Tris base (final 0.25M) (2) 144g Glycine (final 1.92M) (3) pH 8.2-8.4 (4) Add ddH ₂ O to 1000mL
1X Transfer buffer (1L)	(1) 100ml 10X Transfer buffer (2) 200ml Methanol (final 20%) (3) Add ddH ₂ O to 1000mL
10X TBS (Tris buffer saline) (1L)	(1) Tris:24.33g (2) NaCl:80.06g (3) Dissolve all above in 800mL ddH ₂ O (4) Check that pH is 7.6
1X TBST (Tris buffer saline/Tween-20) (1L)	(1) 100ml 10X TBS (2) 5ml Tween 20 (20%)

	(3) Add ddH ₂ O to 1000mL
10X Running buffer (1L)	(1) 30.3g Tris base (final 0.25M) (2) 144g Glycine (final 1.92M) (3) 10g SDS (final 1%) (4) Dissolve all above in 800ml ddH ₂ O (5) Check that pH is 8.3-8.5 (6) Add ddH ₂ O to 1000mL
5% Blocking buffer (50 mL)	(1) 2.5g BSA (2) Add 1xTBST till 50mL
10% APS solution (10 mL)	(1) 1g Ammonium persulphate (2) 10 mL ddH ₂ O
10% SDS solution (100 mL)	(1) 10g SDS (2) 100 mL ddH ₂ O

2.1.10 Software tools and websites

Table 10: Software tools and websites

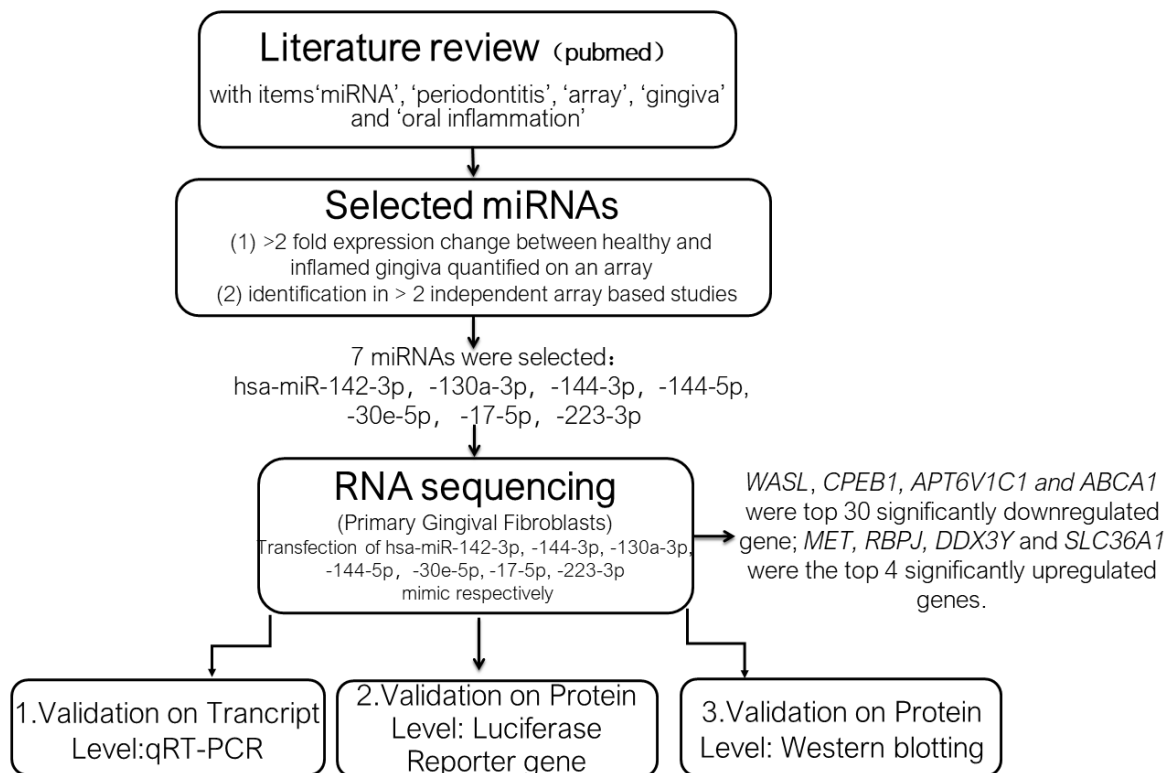
Software tools and websites	Website / software
Biorender	https://www.biorender.com/
CFX Manager Software 3.1 for qRT-PCR cycler	Bio-Rad
Clone Manager 9, Professional, version 9.2	Sci Ed Software LLC.
Ensembl genome browser 104	https://www.ensembl.org/index.html
GraphPad Prism 6, version 6.01	GraphPad
Human protein atlas	https://www.proteinatlas.org/
ImageJ, 1.48v	https://imagej.nih.gov/ij/index.html
IBM SPSS statistics 28.0.1.0	IBM SPSS statistics
LaTex	https://www.overleaf.com/project
miRDB	https://mirdb.org/cgi-bin/search.cgi
miRbase	https://www.mirbase.org/
NEB Tm Calculator, version 1.13.0	https://tmcalculator.neb.com/#!/main
NEBioCalculator, version 1.13.1	https://nebiocalculator.neb.com/#!/ligation
NCBI	https://www.ncbi.nlm.nih.gov/
Office Word, PowerPoint, Excel	Office Word, PowerPoint, Excel
Primer3web, version 4.1.0	https://primer3.ut.ee/

Primer blast	https://www.ncbi.nlm.nih.gov/tools/primer-blast/
TargetScanHuman 7.1	http://www.targetscan.org/vert_71/

2.2 Methods

2.2.1 miRNA selection

Using the search terms 'miRNA', 'periodontitis', 'gingiva', and 'oral inflammation', array-based miRNA expression studies performed in healthy and inflammatory oral tissues (gingiva, saliva) of periodontitis patients were located in the PubMed database of biomedical and life sciences literature. From the results of 26 studies, meta-analyses, reviews and clinical related articles were excluded and original research articles on miRNA array expression profiling studies were included for further analysis (for the workflow of the study, see **Figure 3**). In total, 6 studies were identified (Fujimori et al. 2019; Lee et al. 2011; Ogata et al. 2014; Perri et al. 2012; Stoecklin-Wasmer et al. 2012; Xie et al. 2011). The selection criteria for miRNAs reported by these studies were differential expression found by at least 2 independent miRNA array expression profiling studies with fold change >2 (**Table 11**), and they should have clear specifications of the strand orientation. hsa-miR-142-3p, -130a-3p and -30e-5p fulfilled this condition and were found by 3 independent studies (**Table 11**). Additionally, hsa-miR-144-3p, -144*, -223-3p, and -17-5p were found by 2 independent studies. Since both miRNAs (hsa-miR-144-3p, -144*, -223-3p, -17-5p) had similar expression and we could not distinguish the disease-relevant miRNA, we selected all four of these miRNAs. These studies also provided clear specifications of the strand orientation; therefore, in total, we selected these 7 miRNAs (hsa-miR-142-3p, -130a-3p, -30e-5p, -144-3p, -144*, -223-3p, -17-5p).

**Figure 3.** Workflow of the study**Table 11.** Differentially expressed miRNAs in healthy and inflamed gingival biopsies found in the indicated miRNA array-based studies

miRNA	(Xie et al. 2011)	(Fujimori et al. 2019)	(Lee et al. 2011)	(Stoecklin-Wasmer et al. 2012)	(Perri et al. 2012)	(Ogata et al. 2014)
hsa-let-7a	2-5	-	9.48	-	-	-
hsa-miR-130a	2-5 (-3p and -5p)	-	18.83 (-3p)	-	4.6/6.4 (-3p)	-
hsa-miR-142-3p	2-5	-	-	-	2.4/5.3	2.33
hsa-miR-17-5p	2-5	-	2.37	-	-	-
hsa-miR-302b	2-5	-	9.5	-	-	-
hsa-miR-30e	2-5 (-3p and -5p)	-	2.4 (-5p)	0.66 (-5p)	4.4/4.9 (-5p)	-
hsa-miR-144-3p	-	2.16	9.5	-	-	-
hsa-miR-223-3p	-	-	-	2.53	-	2.73
hsa-miR-210	-	-	-	0.47	1.4/2.3	-
hsa-miR-144*	2-5	-	-	-	-	2.08
hsa-miR-126	2-5	-	-	1.51	-	-

Bold letters indicate the 7 selected miRNAs. Numbers indicate fold change. The strand orientation is given in parentheses if not shown in the first column.

Of the 6 studies, 5 studies (Lee et al. 2011; Ogata et al. 2014; Perri et al. 2012; Stoecklin-Wasmer et al. 2012; Xie et al. 2011) obtained inflamed gingival tissues from periodontitis patients diagnosed by probing depth (PD) > 4 mm, and attachment loss \geq 3 mm. 1 study (Fujimori et al. 2019) collected saliva. One study (Stoecklin-Wasmer et al. 2012) collected both inflamed and healthy gingiva from periodontitis patients. This study and the study of (Ogata et al. 2014) and (Perri et al. 2012) diagnosed bleeding on probing on the day of tissue collection.

2.2.2 Isolation and Cultivation of Primary Human Gingival Fibroblasts (phGFs)

Primary human gingival fibroblasts (phGFs) were isolated from gingival tissues of three different donors. The tissues were washed in 80% ethanol for 30 seconds, rinsed with Dulbecco's Phosphate-Buffered Saline (DPBS), and incubated at 4°C in DMEM medium (+1% penicillin/streptomycin). Type IV collagen and fibronectin were enzymatically digested using neutral protease Dispase II to separate gingival tissues into epithelial cells and fibroblasts. The next day, gingival tissues were separated using forceps. After adding 5 mL of DMEM medium (+1% penicillin/streptomycin, +5% FBS), the solution containing dissociated epithelial tissue was pipetted 80 times using a 5 mL pipette. To remove debris and isolate primary epithelial cells, the solution was passed through a 70 μ m cell strainer placed in a 50 mL Falcon tube, and the cell strainer was gently triturated with a cell scraper. The cell strainer was washed with 20 mL of DMEM medium (+1% penicillin/streptomycin, +5% FBS) and centrifuged at 300 x g for 5 minutes. The supernatant was aspirated, and the cell pellet was resuspended in 5 mL of DermaLife K, a complete supplemented medium, and transferred to T25 cell culture flasks coated with 1 mg/mL of collagen type A.

Small pieces of connective tissue were dissected with a scalpel and placed in 1 mL of DMEM medium (+10% FBS, +1% non-essential amino acids) to promote fibroblast growth. After approximately two weeks, the fibroblasts were passaged in T75 cell culture flasks until they reached the 3rd to 5th passage for miRNA transfection.

Primary human gingival fibroblasts (phGFs) were grown in T75 flasks at 37°C with 5% CO₂ in a humidified incubator. Once the cells reached approximately 90% confluence, they were passaged under aseptic conditions. For this, the culture medium was aspirated from the fibroblasts and cells were washed twice with DPBS. Then, DPBS was removed, and 2 mL of trypsin/EDTA was added to the cells and incubated at 37°C for 5 minutes. To stop trypsin digestion, 10 mL of medium

(DMEM medium + 10% FBS, + 1% non-essential amino acids) was added. Depending on the confluence, 1 to 3 mL of cell suspension was transferred to a fresh T75 cell culture flask and cultured until the cells again reached 90% confluence. phGF cells (3rd to 4th passage) were seeded at a density of 3.0×10^5 cells per well in a 6-well tissue culture plate one day before transfection.

2.2.3 miRNA transfection

Three technical duplicates of three donors' phGFs from unrelated healthy donors were separately transfected with mirVana miRNA mimics miR-144-3p, -144-5p, -142-3p, -130a-3p, -30e-5p, -17-5p and -223-3p, respectively. The negative control mirVana miRNA Mimic Negative Control #1 was used for sample normalization. As a positive control, phGFs were transfected with the mirVana miRNA mimic miR-1, which downregulates the expression of the gene *PTK9* (Protein Tyrosine Kinase 9). The medium needs to be changed before transfection. By using Lipofectamine RNAiMAX reagent, the miRNAs were transfected. For each transfection, the reaction was as follows:

Step 1: 9 μ L Lipofectamine RNAiMAX reagent + 141 μ L Opti-Mem Medium

Step 2: 3 μ L mirVana miRNA mimic (30 pmol) + 147 μ L Opti-Mem Medium

Step 3: Two reactions were gently mixed by adding the second reaction to the first and incubated for 5 minutes at room temperature. 250 μ L miRNA-lipid combination was then added to each well of cells. After transfection for 24 hours, the cells were washed twice with DPBS.

2.2.4 Total RNA extraction

After 24 hours of transfection, total RNA was extracted from phGFs. The culture medium was aspirated from the 6-well cell culture plate and cells were washed twice with 1x DPBS. At the final wash stage, DPBS was removed, and 350 μ L of lysis buffer containing 3.5 μ L of β -mercaptoethanol was added to each well to get complete cell lysis. Cells were detached from the bottom of the plate using a cell scraper and the entire cell lysate was transferred to QIAshredder spin columns and centrifuged at 14,000 x g for 3 minutes. Afterwards, RNA extraction was performed using the RNeasy Mini Kit. Samples were thawed on ice, and an equal volume of 70% ethanol was added. Then, the columns were centrifuged for 30 seconds at 14,000 g (room temperature), and RNA adhered to the silica membrane, while other cellular components in the solution were removed as the flow-through. After washing with 350 μ L of wash buffer, DNase-I digestion was performed on the column at room temperature (RT) for 15 minutes using DNase-I (70 μ L RDD buffer + 10 μ L DNase I) to prevent genomic DNA contamination of the RNA. After multiple

washes to remove the remaining salt impurities in the column, RNA was eluted in 35 µL of ultrapure water (UPW), and its concentration was measured using the Multiskan GO Spectrophotometer. The RNA quality was determined by the 260/280 ratio, which should be in the range between 1.9-2.1. Subsequently, all RNA was stored at -80°C for further use.

2.2.5 RNA sequencing (RNA-seq)

Using the NextSeq 500/550 High Output Kit v2.5, 500–1,000 ng total RNA from transfected cell cultures were sequenced with 16 million reads (75 bp single end) on a NextSeq 500 (Illumina). The Berlin Institute of Health's Genomics Core Facility conducted the RNA-Seq. STAR aligner version 2.7.5a was used to align reads to the human genome sequences (build GRCh38.p7) (Dobin et al. 2013). Using the multiqc reporting tool (Ewels et al. 2016), the readings' quality control (QC) was examined. This included fastqc (which is accessible at <http://www.bioinformatics.babraham.ac.uk/projects/fastqc>), dupradar (Sayols et al. 2016), and qualimap (DeLuca et al. 2012). The STAR software was used to obtain the raw counts. Analysis of differential gene expression has recently been reported (Chopra et al. 2022). In short, we employed the CERNO test from the tmod package (Zyla et al. 2019), version 0.46.2, and MSigDB for gene set enrichment analysis, as well as the R package DESeq2 (Love et al. 2014), version 1.26.(Liberzon et al. 2015). The goseq package, version 1.38 (Young et al. 2010), was used for the hypergeometric test and the Gene Ontology gene sets. The Benjamini-Hochberg correction was used to adjust the P-values for the genes with differential expression for multiple testing. The q values for the revised P-values are provided (false discovery rate [FDR]).

I utilized the internet database miRDB to estimate the miRNAs' target genes (Chen and Wang 2020). We utilized the online tool TargetScanHuman (version 7.1) to find miRNA binding sites inside the 3'UTRs of the anticipated miRNA target genes. For each miRNA, the list of substantially differentially regulated genes ($P_{adj} = 0.05$) was first sorted by target score > 80 to identify regulatory candidate genes. Subsequently, the list was sorted by ascending $\log_2 FC$.

2.2.6 qRT-PCR

2.2.6.1 RNA purification

RNA purification was achieved by performing additional DNase I digestion to eliminate any traces of DNA in the total RNA. To accomplish this, the TURBO DNA-free Kit was used according to the manufacturer's instructions. For the preparation of RNA from the 6-well plates, a two-step TURBO rigorous DNase treatment was performed. The reaction involved 30 µL of total RNA, 5 µL of 10X TURBO DNase buffer, and 2 µL (4 U) of TURBO DNase. Initially, the mixture was

incubated at 37°C for 30 minutes, followed by the addition of an additional 1 µL (2 U) of TURBO DNase and another 30 minutes of incubation at 37°C. The reaction was terminated by adding 10 µL of TURBO inactivation reagent at room temperature for 5 minutes. Subsequently, the samples were centrifuged at 14,000 × g for 1.5 minutes, and the supernatant was transferred to a new tube. The RNA was then purified and used for reverse transcription. Finally, a PCR was performed using plasmid backbone primers and a pGL4.24 DNA template as a positive control to ensure complete removal of DNA.

2.2.6.2 cDNA synthesis

The process of synthesizing complementary DNA (cDNA) from an RNA template through reverse transcription is referred to as cDNA synthesis. In this process, oligo dT primers were utilized, which bind to the poly-A tail of eukaryotic mRNA. Mix the whole 20µL reaction system as described below: 6µL (500 ng) RNA, 1 µL dNTPs, 1 µL oligo dTs, 6 µL UPW, 2 µL 10 x reverse transcriptase buffer, 1 µL RNase inhibitor, 1 µL Multiscribe reverse transcriptase. Then, put the mixed sample into the PCR machine, choosing the program for cDNA synthesis (for program details, see **Table 12**).

Table 12: PCR program of cDNA synthesis

Steps	Temperature (°C)	Time (min)
1	25.0	10: 00
2	37.0	120: 00
3	85.0	05: 00
4	4.0	Pause
Total run time	-	2h16min

2.2.6.3 qRT-PCR primer design

The primer design software primer3 (<https://primer3.ut.ee/>) and NCBI primer blast (<https://www.ncbi.nlm.nih.gov/tools/primer-blast/>) were used for primer design. The desired length of the amplicons was set between 70 bp and 250 bp, and the annealing temperature for all primers was set at 60°C. Whenever possible, primers were designed to span exon-exon junctions, with one primer crossing the exon-intron boundary. In cases where it was not possible to span the

exon-exon junction, primers were selected to be located in different exons with a long intron between them. The use of primers spanning exon boundaries was particularly favored as it helps minimize amplification of genomic DNA and prevents false-positive amplification.

2.2.6.4 qRT-PCR

Quantitative real-time polymerase chain reaction (qRT-PCR) is a method used to quantify nucleic acid and gene expression. It involves amplifying cDNA. SYBR Green I, a fluorescent dye that binds to the cDNA double helix and emits light at 520 nm, was utilized in this study. The fluorescence signal increases with each cycle as the cDNA amplicons grow. The CFX Connect Real-Time PCR Detection System, equipped with three LEDs that emit light at an excitation wavelength of 450-480 nm (matching the excitation wavelength of SYBR Green: 497 nm), was employed. The SYBR Green Master Mix used in this study contains the necessary components, including SYBR Green I dye, dNTPs, Ampli Taq Gold polymerase, and an appropriate buffer, to ensure optimal reaction conditions. The reaction mixture consisted of 1 µL of cDNA, 5 µL of SYBR Green Master Mix, 0.02 µL of forward primer (100 µM), 0.02 µL of reverse primer (100 µM), and 3.96 µL of ultrapure water (UPW), resulting in a total volume of 10 µL. qRT-PCR was performed using the CFX Connect Real-Time PCR Detection System, and the specific amplification program details can be found in Table 13. The Ct value was obtained from each sample, which can be used to determine the amount of target input. The $2^{-\Delta\Delta CT}$ method enables relative quantification. The specificity of qRT-PCR products can be confirmed by examining melt or dissociation curves.

Table 13: qRT-PCR program

No.	Temperature (°C)	Time (min)	Steps
1	50	02:00	Activation
2	95	02:00	Initial denaturation
3	95	00:15	Denaturation
	60*	01:00	Annealing Extension
4	-	-	35 cycles starting with No. 3
	95	00:05	
5	65	00:05	Melting curve analysis
	95	00:50	

2.2.7 Cloning of *CPEB1* 3'UTR sequence into the reporter plasmid pGL4.24

2.2.7.1 Polymerase chain reaction (PCR)

We chose the periodontal risk gene *CPEB1* (Cytoplasmic Polyadenylation Element Binding Protein 1), which was downregulated by miR130a-3p, to show how miRNA regulation affects a target gene mechanistically. Three conserved 7mer sites in *CPEB1*-3'UTR match the seed region of hsa-miR-130a-3p. Primers of *CPEB1*-3'UTR were designed by using Primer 3 (described above in Chapter 2.2.6.3), which contained two types of enzyme sites (XbaI and FseI). In the reporter vector pGL4.24 (Promega), we cloned 920 basepairs (bp) of the *CPEB1* 3'UTR sequence, including the miRNA binding sites, upstream of the Luc polyadenylation site. With the use of Qiagen's AllPrep DNA/RNA/miRNA Universal Kit, and the template DNA named genomic DNA (gDNA) that was isolated from phGFs, DNA was amplified by PCR using Phusion High-Fidelity PCR Polymerase (NEB) to amplify the 3' UTR of *CPEB1*, and the following PCR reaction was performed: 4 µL 5 x Phusion HF Buffer, 0.4 µL 10 mM dNTPs, 1 µL fwd-Primer (10 µM), 1 µL rev-Primer (10 µM), 1 µL Template DNA (genomic DNA; 100-200 ng), 0.2 µL Phusion polymerase, 12.4 µL UPW; Gently mix the 20µL volume combination. Move the tubes into the PCR machine and start the PCR program. The PCR program is given in **Table 14**.

Table 14: PCR program for 3'UTR of CPEB 1

Steps	Temperature	Time	Cycle
1	98°C	05:00	Activation
2	98°C	00:10	Denaturation
3	71°C	00:30	Annealing
4	72°C	01:00	Elongation (to step 2 with 35 cycles)
5	72°C	10:00	-
6	4°C	Pause	-

2.2.7.2 Restriction digest

The 920-bp sequence, encompassing three 7-mer sites, was inserted into the 3' untranslated region (UTR) of the reporter vector pGL4.24, specifically at the adenylation sites within the firefly luciferase gene. The 3' UTR sequence of *CPEB1*, spanning 920 nucleotides, was amplified using PCR. Subsequently, both the PCR product and the pGL4.24 plasmid were digested with XbaI and FseI restriction enzymes. The reaction mixture, comprising 2 µL of DNA (~2 µg PCR product/pGL4.24), 1 µL of XbaI, 1 µL of FseI, 5 µL of 10x rCutSmart buffer, and 41 µL of ultrapure water (UPW), was prepared to a final volume of 50 µL. The reaction mixture was incubated at 37°C for 2-3 hours, followed by loading onto a 1% agarose gel, as described in Section 2.2.7.3. Finally, the restricted plasmid DNA was isolated from the 1% agarose gel, following the procedure outlined in Section 2.2.7.4.

2.2.7.3 Gel electrophoresis

To determine the size of DNA fragments generated during PCR or restriction digestion, gel electrophoresis was employed. This method separates DNA fragments based on their size by applying an electric field through an agarose gel. Typically, agarose gels with concentrations ranging from 1% to 2% are used. For a 1% agarose gel, 4.0 g of agarose powder was dissolved in 400 mL of 1xTAE buffer by carefully heating it for 30 minutes. From this, 200 mL of 1% gel was transferred into a new Falcon tube, followed by the addition of 5 µL of ethidium bromide. 50 µL of DNA, which was mixed with a 6x orange loading dye, was finally loaded into each well on the gel. To determine the size of DNA bands in the gel, 5µL DNA markers (GeneRuler 1 kb Plus DNA Ladder or 50 bp O'Range Ruler) were also loaded in the gel. An electric voltage of 110 V was applied for 45 minutes (**Figure 4**) to facilitate the migration of DNA fragments.

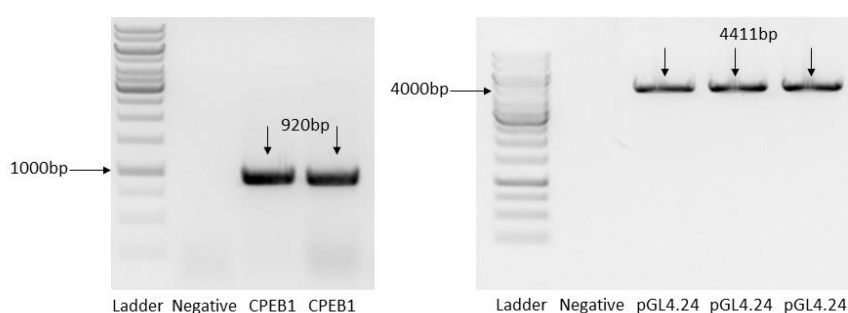


Figure 4. 1% agarose gel picture of restricted PCR product of *CPEB1* 3' UTR on the left and restricted pGL4.24 vector on the right. The electrophoresis was carried out at 110 V for 45 minutes. The identified DNA fragments were extracted from the gel following the method outlined in Chapter 2.2.8.

2.2.8 Purification of DNA fragments

The QIAquick Gel Extraction Kit was utilized to purify the DNA fragments from the agarose gel. Initially, the suitable DNA bands were excised from the gel using a scalpel and weighed. Subsequently, 300 µL of QC buffer was added to the DNA fragments for every 100 mg gel and the combination was incubated at 50°C for 10 minutes. After the agarose gel was completely dissolved, the entire contents were pipetted onto a new column and centrifuged at 14,000 x g for 1 minute. In this step, the high salt concentration of the previously added buffer caused the DNA to adsorb onto the silica membrane of the column, while primers, enzymes, and other contaminants were discarded as supernatant. The excess salts were removed by washing the DNA with 750 µL of wash buffer, and finally, it was eluted with 30 µL of UPW. The DNA concentration was measured using the Multiskan GO Spectrophotometer. The quality of the DNA was assessed based on the 260/280 ratio, which should ideally fall between 1.7 and 2.0. Subsequently, all the DNA samples were stored at -20°C for future use.

2.2.9 Ligation

DNA ligation is the process of creating a phosphodiester bond between two single strands of DNA or linearized plasmid DNA. This bond is formed through the catalytic action of a ligase, which connects the 3'-hydroxyl end of the PCR products with the 5'-phosphate end of the restricted plasmid DNA, resulting in the formation of a phosphodiester bond.

To clone the reporter gene plasmids, the following ligation reactions were performed: 2µL of pGL4.24 (restricted by XbaI and FseI) (50 ng), 1.5 µL of PCR product (restricted by XbaI and FseI) (37.5 ng), 2 µL of T4 ligation buffer, 1 µL of T4 ligase, and 13.5 µL of UPW (the total volume of the reaction mixture is 20 µL). Following an overnight incubation of the ligation reaction at 16 C, the transformation into competent cells was carried out according to the procedure described in Chapter 2.2.10.

2.2.10 Transformation

Transformation refers to the uptake of DNA by competent bacterial cells. In this study, for the purpose of transformation, 100 µL of self-prepared competent Top10 Escherichia coli cells (NEB) were slowly thawed on ice for 10 minutes, followed by incubation on ice with 10 µL of the ligation mixture for 20 minutes. Subsequently, a heat shock was performed by heating the cells at 42°C for 50 seconds, followed by a 3-minute placement on ice to allow the plasmid DNA to enter the cells. After this, 300 µL of SOC medium was added inside, and the cell mixture was incubated at 37°C with shaking at 250 rpm for 50 minutes. Finally, the cell mixture was plated on YT agar plates supplemented with 100 mg/mL ampicillin (amp) and incubated overnight at 37°C. Single colonies

were picked and checked via colony PCR (described in Section 2.2.7.1), and then grown overnight in 8 mL of YT medium supplemented with amp (100 mg/mL).

Plasmid DNA was isolated using the procedure described in Section 2.2.11.

2.2.11 Plasmid DNA isolation

The QIAGEN Plasmid Mini Kit and QIAGEN Plasmid Midi Kit were utilized to isolate the plasmid DNA from the bacterial cell pellet obtained from an 8 mL overnight culture, which was centrifuged at 7,000 x g for 15 minutes at room temperature. The bacterial pellet was initially resuspended in 250 μ L of pre-cold resuspension buffer P1 (composed of 50 mM Tris-HCl, pH 8.0, 10 mM EDTA, and 100 μ g/mL RNase A) and transferred into a 1.5ml microcentrifuge tube. Next, 250 μ L of lysate buffer P2 (comprised of 200 mM NaOH and 1% SDS) was added to the bacterial cell suspension, and the mixture was inverted 4-6 times. Then, the 350 μ L buffer N3 was added into the mixture with 4-6 times inverting. Afterwards, the supernatant (DNA solution) was loaded onto the column and centrifuged at 13,000 rpm for 10 minutes (room temperature). The DNA was rinsed using 0.75 mL of alcohol-containing PE buffer to remove the remaining buffer and salt residues from the column, followed by centrifugation at RT and 13,000 rpm for 1 minute. The DNA was eluted using 35 μ L UPW and collected in a 1.5 mL clean tube by centrifugation for 1 min at 13,000 rpm. To measure the concentrations of DNA, a Multiskan Go spectrophotometer was used. For this purpose, 2 μ L of the standard (UPW) and sample solution were pipetted onto the drop plate. Each measurement utilized two templates, and the absorbance of DNA solutions was measured at 260 nm. Subsequently, all the plasmid DNA samples were stored at -20°C for future use.

2.2.12 DNA sequencing

At LGC Genomics GmbH (Berlin), plasmid DNA sequencing was carried out to verify the correct cloning sequence of *CPEB1*-3'UTR into vector. A volume of 15 μ L containing 100ng/ μ L of plasmid DNA was submitted to the company. Using Clone Manager 9.0 software, sequence alignments were produced (**Figure 5**). The correct plasmid DNA was stored at -20°C for future use.

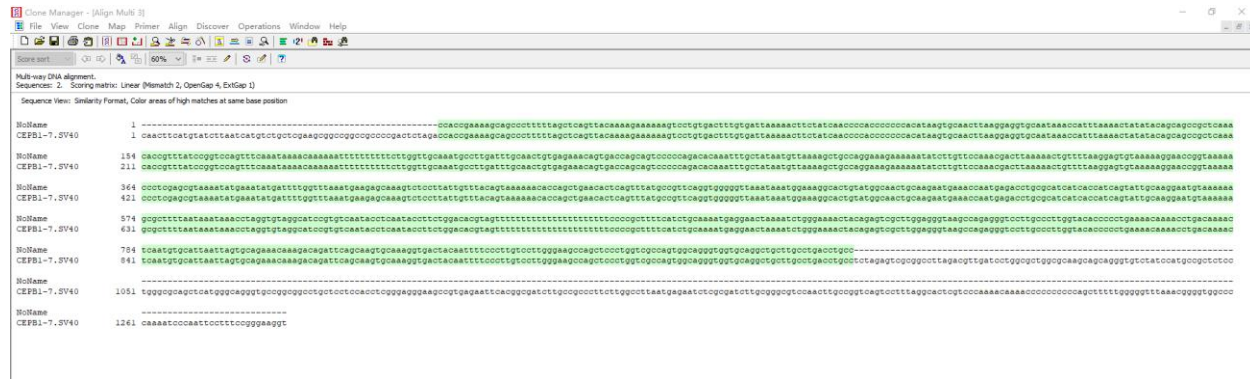


Figure 5. Sequence alignment of *CPEB1*-3'UTR. The initial line displays the *CPEB1* reference sequence, while the subsequent line exhibits the *CPEB1* sequence that was amplified from genomic DNA and cloned into the pGL4.24 plasmid. The 3' UTR region of *CPEB1* is indicated in green, and regions of matched sequences at identical base pair positions are shaded.

2.2.13 Co-transfection of plasmid DNA and miRNAs

2.2.13.1 Cultivation of ihGFs for reporter gene assays and Western Blotting

Immortalized Human Gingival Fibroblasts (ihGFs, ABM) were used for reporter gene assays. ihGFs were cultivated in a T75 flask at 37°C in a 5% CO₂ incubator. Prior to cell passage, cell confluence had attained approximately 90 %. To achieve this, the medium from the confluently grown cells was extracted, and the cells were rinsed twice with DPBS. The DPBS was then removed, and the cells were incubated at 37°C for 2 minutes with 3 mL of Trypsin/EDTA. By adding 5 mL of culture medium (DMEM media (+ 10% FBS, + 1% non-essential amino acids (NEAA)), the trypsinization of ihGFs was halted. The cells were then transferred to a 50 mL falcon and centrifuged for five minutes at 300 x g (room temperature). The supernatant was then extracted, and the cells were resuspended in 2 mL of fresh culture medium. Depending on the confluence of the cells, the entire cell suspension was transferred to a new T175 cell culture vial containing 30 mL of culture medium and incubated until the cells reached 90% confluence once again.

2.2.13.2 Transfection of ihGFs with dual reporter gene plasmids

In 6-well cell culture plates, ihGF cells were inoculated with 180,000 cells per well one day prior to transfection. There were always three independent biological replications of transfected cells. Before transfection, the medium of the cells was changed. Lipofectamine 2000 and Lipofectamine RNAiMAX Transfection Reagent (Thermo Fisher Scientific) were used to transfect cells with the dual reporter gene plasmids and miRNA mimics. One 6-well's transfection reactions were as follows:

1. Reaction: 1.3 µL (2.7 µg pGL4.24- *CPEB1* and 0.3 µg Renilla) DNA + 148.7 µL Opti-mem
 2. Reaction: 6 µL lipofectamine 2000 + 144 µL Opti-mem

Gently mix both reactions, add reaction B into A, then gently vortex and centrifuge. Incubate for 20 min at RT. Add 250 µL into each well. Change the culture medium after 4h. After 24h incubation, change the fresh medium prior to transfection of the miRNAs into the cells. For the detailed transfection protocol, see below:

1. Reaction: 3µL miRNA mimics + 147 µL Opti-mem
2. Reaction: 9µL Lipofectamine RNAiMAX + 141 µL Opti-mem

Gently mix both reactions, add reaction B into A, incubate for 5min at RT, then add 250 µL into each well. After transfection for a further 24 hours, the cells were rinsed twice with PBS. As described in next chapter, further Luciferase reporter gene assays were performed.

2.2.14 Luciferase Reporter gene assays

MicroRNAs (miRNAs) target mRNA at particular locations in the 3'UTR to cleave targets or hinder translation. An RNA-induced silencing complex (RISC) mediates the miRNA-target interaction, which relies on sequence complementarity and the number of binding sites in a 3' UTR. To achieve this, the *CPEB1* 3'UTR are cloned into downstream of a firefly luciferase reporter. After plasmid DNA and miRNAs are co-transfected into ihGFs, the reporter expression is monitored. Luciferase levels can reveal if a miRNA can bind to the 3'UTR and control its expression. The Dual-Luciferase Reporter Assay System was used to allow the measurement of two reporter enzymes from one sample: the Firefly luciferase, which was downstream of the 3'UTR, and the Renilla luciferase, which served as an internal control. To control for experimental variability, plasmid pGL 4.24, which expresses the Renilla luciferase, was used.

After co-transfection of plasmid DNA and miRNA mimics, cells were rinsed with cold DPBS and treated for 15 min with 1 x Passive lysis buffer on a rocking platform at room temperature. 5 µL of cell suspension from each group was pipetted onto a 96-well plate. An Orion II Microplate Luminometer (Berthold, Germany) was used to measure the results. For each test, the luminometer performed a 2-second premeasurement delay and a 10-second measurement. Each sample received 25 µL of luciferase assay reagent II (LAR II) and 25 µL of Stop&Glo reagent. Relative fold changes (FC) in activities were computed by dividing the average (Firefly/Renilla) of the experimental group (co-transfection of plasmid *CPEB1* and miR-130a-3p) by the average (Firefly/Renilla) of the negative control group (co-transfection of plasmid *CPEB1* and miRNA negative control). GraphPad Prism 6 was used to determine differences in protein levels using a t-test (GraphPad Software, Inc.).

2.2.15 Quantitative reverse transcription polymerase chain reaction (qRT-PCR)

To confirm that hsa-miR-130a-3p inhibits the target mRNA at the transcript level, qRT-PCR was utilized to measure the expression of the reporter gene following co-transfection of Plasmid DNA

and miRNA mimics. RNA isolation, RNA purification, cDNA synthesis and qRT-PCR were performed by the same protocol mentioned above in Chapter 2.2.6. Prior to this, by using pGL4.24 backbone primers, a PCR was performed on the cDNA to assess for genomic DNA contamination, and DNase I digestion was carried out until no genomic DNA was detectable, as depicted in **Figure 6**.

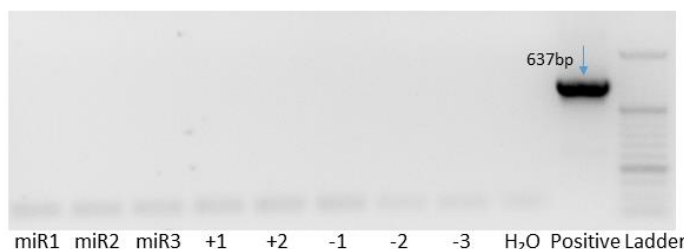


Figure 6. 1% agarose gel picture of PCR to check genomic DNA contamination of cDNA. No PCR product was obtained. This meant that the total RNA could be used in the next qRT-PCR step.

By measuring *PTK9* transcript levels prior to checking the Luc gene activity, we were able to ascertain the transfection effectiveness and functioning of the miRNA positive control mimic. For the primers of *PTK9*, *LUC*, and *GAPDH*, see **Table 8.2**.

For the quantification of *MET*, *RBPJ*, *DDX3Y* and *SLC36A1* genes' activity, after transfection of miR-130a-3p, -142-3p, -144-5p, -144-3p, -30e-5p, 17-5p, and -223-3p, total RNA was isolated from transfected phGFs. 500 ng of the total RNA was transcribed into cDNA as described in Chapter 2.2.6.2. Differential expression of the *MET*, *RBPJ*, *DDX3Y* and *SLC36A1* genes was quantified by qRT-PCR with primers of *MET*, *RBPJ*, *DDX3Y* and *SLC36A1* (**Table 8.2**) .

Ct values of the tested genes were normalized to *GAPDH* Ct values. Fold changes of relative gene expression were calculated by the $2^{-\Delta\Delta Ct}$ method. All of these gene transcript levels were compared between ihGFs/ phGFs that were transfected with the positive and negative control mimics. Differences of transcript levels were analysed with a t-test.

2.2.16 Protein expression analysis

2.2.16.1 Protein extraction

24 hours after plating 3.0×10^5 ihGFs per well in a 6-well plate, the cells were transfected by miRNA mimics for another 24 hours. Once plates were rinsed with cold PBS, RIPA buffer was added for 15 minutes (50 mM Tris-HCl, pH 7.4, 150 mM NaCl, 0.5 mM MgCl₂, 0.2 mM EDTA, and 1% Triton X-100 with protease inhibitor cocktail (Thermo Scientific). Cells were removed

and samples were clarified by centrifugation for 15 minutes at 14,800 g and at 4°C. For future use, the proteins were stored in a -80°C freezer.

2.2.16.2 Protein concentration measurement

According to the manufacturer's instructions, a BCA Protein Assay reagent (Pierce) was used to determine protein concentration. To draw a standard curve and add samples according to the **Table 15**. The detailed procedure stages are as follows:

Table 15: Standard curve measurement

Well	0	1	2	3	4	5	6	7
BSA(0.5μg/μl)	0	1	2	4	8	12	16	20
H ₂ O(μl)	20	19	18	16	12	8	4	0

Configure an adequate quantity of BCA working agent based on the total amount of samples according to a volume ratio of BCA reagent A and B solution of 50:1, mix thoroughly, and add 200μl of the mixed BCA buffer to each well above. After thorough mixing, incubate at 37°C for 30 minutes, perform colorimetry at 562nm, document the absorbance value of each space, and construct a standard curve (the abscissa represents protein concentration (ug) and the ordinate is the absorbance value). Add 20μl of the diluted sample to each well, then add the BCA mixture, mix thoroughly, incubate at 37°C for 30 minutes, perform colorimetry at 562nm, and document the absorbance value of each space. On the basis of the absorbance value of the measured sample, the corresponding protein amount (μg) can be found on the standard curve, and the sample's actual concentration can be calculated using the following formula:

$$\text{Final protein concentration}(\mu\text{g}/\mu\text{l}) = \text{protein amount } (\mu\text{g}) / 20 \times 10.$$

Adjust the concentration of various samples to the same level prior to electrophoresis using RIPA lysis buffer.

2.2.17 Western Blotting

2.2.17.1 Protein Sample Preparation

Add the obtained protein sample mentioned above to 6x sample loading buffer in a volume ratio of 5:1, boil it at 95°C for 10 minutes, and aliquot the sample for further experiments.

2.2.17.2 SDS-PAGE

According to the molecular weight of the target protein, a separation gel with a concentration of 10% or 6% and a stacking gel with a concentration of 6% or 4% should be selected, and the liquid should be prepared according to **Table 16**.

Table 16: SDS page preparation chemicals

Chemicals	Protein weight > 100kDa		Protein weight < 80kDa	
	6%Separation Gel	4%Stacking Gel	10%Separation Gel	6%Stacking Gel
H ₂ O (ml)	5.3	2.4	4.0	2.1
30%Acrylamide (ml)	2	0.5	3.3	0.5
1.5M TrisHCl (pH 8.8) (ml)	2.5	-	2.5	-
1M TrisHCl (pH 6.8) (ml)	-	1	-	0.38
10%SDS (μl)	100	40	100	30
10%APS (μl)	100	20	100	30
TEMED (μl)	10	4	10	3

Fix the 1cm thick glass plate, first adding 3ml of separating gel to the center of the glass plate. Then, add 1ml of isopropanol to flatten the liquid surface and isolate any air bubbles. Wait for 15 minutes until the separating gel is solidified, and then pour off the isopropanol. Next, add 1.5ml of concentrated gel and quickly insert the supporting comb. After the concentrated gel is solidified, move the glass plate into the electrophoresis tank, add 500ml of electrophoresis liquid, and then pull out the comb. Finally, add 30μl of the sample from 2.2.16.1 to each well. Add 7μl protein ladder to the outer wells to mark the positions of the proteins. Connect the power supply and run the electrophoresis at a constant current of 40mA. Stop the electrophoresis when the bromophenol blue reaches the bottom of the gel.

2.2.17.3 Protein transfer

As the electrophoresis is about to end, prepare a PVDF membrane of appropriate size and soak it in formaldehyde for 5 minutes. After electrophoresis, carefully remove the gel, and discard the stacking gel and the gel bottom containing bromophenol blue. Prepare the electrotransfer clips in the order specified in **Table 17**. Add 500ml of transfer buffer to the electrophoresis tank and place

an ice box inside. Transfer the proteins to the membrane at a constant pressure of 100V for 90 minutes, using an external ice bath.

Table 17: The order of the transfer sandwich

Order	Red side
6	Splint (white) and white sponge
5	Filter paper
4	PVDF membrane
3	Gel
2	Filter paper
1	Splint (black) and white sponge
-	Black side

2.2.17.4 Immunoblotting

After transferring the proteins to the PVDF membrane, wash the membrane twice with 1xTBST. Block the membrane with 5% BSA-TBST solution at room temperature for 2 hours, wash three times with 1xTBST again, and then incubate the membrane with the prepared primary antibody at a concentration of 1:2000 overnight at 4°C. Wash the membrane with 1x TBST three times for 10 minutes each time, and then incubate with the prepared secondary antibody (1:5000) at room temperature for 1 hour. Wash the membrane again three times with 1xTBST for 10 minutes each time. Finally, add the prepared developing solution (ECL Western Blotting Substrate) dropwise to the membrane, let it react for 10 seconds, and then capture the image using an imaging system. Save the image in the Tiff format.

3. Results

3.1 Contrast results for differentially expressed miRNAs find periodontitis risk genes as miRNA target genes

To identify the target genes and gene sets of the selected miRNAs that showed increased expression in periodontal inflammation, we overexpressed miRNA mimics in primary human gingival fibroblasts. Upregulation of hsa-miR-130a-3p influenced the expression of 1,819 genes with $P_{adj} < 0.05$. Of these genes, 315 had a predicted hsa-miR-130a-3p binding site, of which 272 showed reduced expression and 48 showed increased expression (**Figure 7**). 1,503 differentially expressed genes had no predicted hsa-miR-130a-3p binding site, 433 of which showed reduced expression and 1,070 genes showed increased expression. The gene *ENPP5* (Ectonucleotide pyrophosphatase/phosphodiesterase family member 5) showed the strongest downregulations, with a fold change (FC) reduction of 5.8 ($\log_2 FC = -2.5$; $P_{adj} = 6.9 \times 10^{-12}$) and a miRNA target score of 96. Periodontitis risk gene *CPEB1* (Cytoplasmic polyadenylation element binding protein 1) (Rhodin et al., 2014) was the second most downregulated gene, showing 2.8 fold downregulation ($\log_2 FC = -1.5$, $P_{adj} = 1.7 \times 10^{-21}$). This gene had the highest target score (100) for hsa-miR-130a-3p binding (**Table 18**).

Upregulation of hsa-miR-142-3p influenced the expression of 2,203 genes ($P_{adj} < 0.05$). 252 genes had a predicted hsa-miR-142-3p binding site, of which 241 showed reduced expression and 11 showed increased expression. The gene *WASL* (WASP Like Actin Nucleation Promoting Factor (*NWASP*)) showed the strongest downregulation ($\log_2 FC = -2.78$, $P_{adj} = 7.1 \times 10^{-140}$, target score = 94). Reduced *WASL* expression is reported to increase the production of inflammatory cytokines in phGFs (Wang et al. 2020).

Upregulation of hsa-miR-144-3p influenced the expression of 19,647 genes ($P_{adj} < 0.05$). Of these genes, 449 had a predicted hsa-miR-144-3p binding site, of which, 420 showed reduced expression and 29 showed increased expression. The gene *UBE2D1* (Ubiquitin Conjugating Enzyme E2 D1) showed the strongest downregulation with $\log_2 FC$ of -2.3; $P_{adj} = 3.7 \times 10^{-4}$), which has been reported to be target gene of miR-144-3p (Li et al. 2021). The gene *NACC2* (NACC Family Member 2) showed the second strongest downregulation ($\log_2 FC = -2.2$, $P_{adj} = 4.9 \times 10^{-56}$). The 4th most differentially regulated gene was *FBN2* (Fibrillin 2) ($\log_2 FC = -2.09$, $P_{adj} = 1.2 \times 10^{-46}$), a known regulatory target of this miRNA (Mo et al. 2021). Notably, the 10th and the 29th most differentially regulated genes, *MAPK6* (Mitogen-Activated Protein Kinase 6) and periodontitis risk gene *ABCA1* (ATP Binding Cassette Subfamily A Member 1), were known target genes (de Aguiar Vallim et al. 2013; Wu et al. 2019).

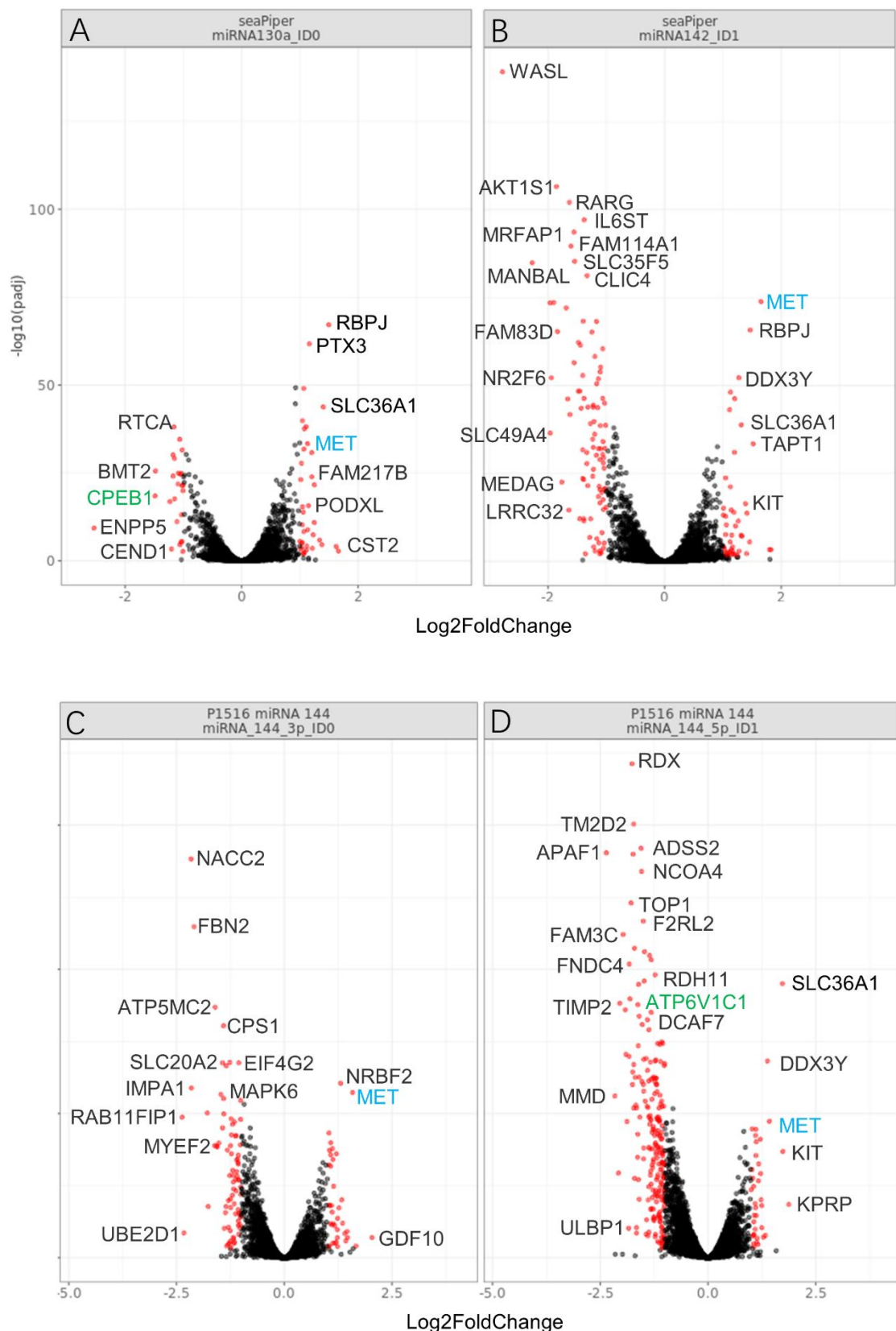
Upregulation of hsa-miR-144-5p influenced the expression of 19,647 genes ($P_{adj} < 0.05$). Of these genes, 129 had predicted hsa-miR-144-5p binding sites, of which, 128 showed reduced expression and 1 (*DPYD*) showed increased expression. The gene *MMD* (Monocyte to macrophage differentiation associated) showed the strongest downregulation ($\log_2 FC = -2.16$, $P_{adj} = 3.7 \times 10^{-23}$). The 4th most downregulated gene was the periodontitis risk gene *ATP6V1C1* (ATPase H⁺ Transporting V1 Subunit C1) (Munz et al. 2019). This gene is a previously reported target of hsa-miR-144-5p (Capstone Project: Data Science DSC180B; Genetic Overlap between Alzheimer's, Parkinson's, and healthy patients; replication project for the paper (Burgos et al. 2014).

Upregulation of hsa-miR-30e-5p influenced the expression of 1,113 genes ($P_{adj} < 0.05$). Of these genes, 365 had predicted hsa-miR-30e-5p binding sites, of which, 358 showed reduced expression and 7 showed increased expression. The gene *IDH1* (Isocitrate dehydrogenase (NADP(+)) 1) showed the strongest downregulation ($\log_2 FC = -2.20$, $P_{adj} = 9.0 \times 10^{-35}$). The 8_{th} most downregulated gene was *ADAM19* (ADAM Metallopeptidase Domain 19). This gene is a previously reported target of hsa-miR-30e-5p.

Upregulation of hsa-miR-17-5p influenced the expression of 880 genes ($P_{adj} < 0.05$). Of these genes, 358 had predicted hsa-miR-17-5p binding sites, of which, 336 showed reduced expression and 21 genes showed increased expression. The gene *ENPP5* (Ectonucleotide Pyrophosphatase/Phosphodiesterase Family Member 5) showed the strongest downregulation ($\log_2 FC = -2.53$, $P_{adj} = 1.9 \times 10^{-09}$). The 4th most downregulated gene was *TGFBR2* (Transforming Growth Factor Beta Receptor 2). This gene is a previously reported target of hsa-miR-17-5p.

Upregulation of hsa-miR-223-3p influenced the expression of 852 genes ($P_{adj} < 0.05$). Of these genes, 131 had predicted hsa-miR-223-3p binding sites, of which, all showed reduced expression and 0 genes showed increased expression. The gene *ARL6IP1* (ADP Ribosylation Factor Like GTPase 6 Interacting Protein 1) showed the strongest downregulation ($\log_2 FC = -1.938$, $P_{adj} = 1.5 \times 10^{-27}$). The 3rd most downregulated gene was *PARP1* (Poly(ADP-Ribose) Polymerase 1). This gene is a previously reported target of hsa-miR-223-3p.

Remarkably, the periodontitis risk genes *CPEB1*, *ABCA1* and *ATP6V1C1* were among the most differentially expressed genes of the miRNAs hsa-miR-130a-3p, hsa-miR-144-3p and hsa-miR-144-5p, respectively.



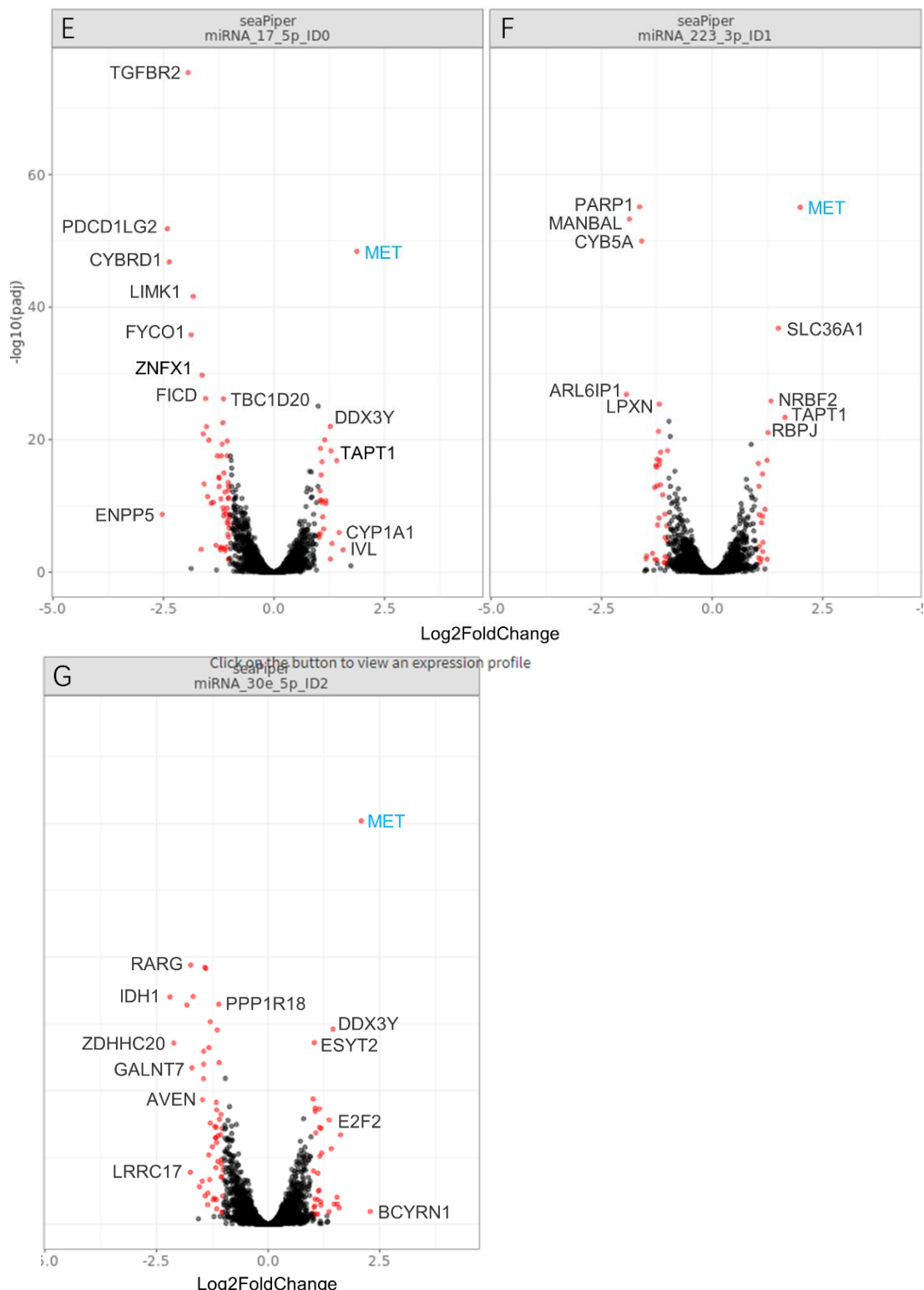


Figure 7A-G. Volcano plots for different differentially regulated genes after miRNA transfection into phGFs. (**Bold = reported miRNA target gene, Green = reported periodontitis risk gene**). Increased levels of each of the 7 selected miRNAs correlated with increased expression of the gene *MET* (color in blue).

Table 18: The 10 most downregulated genes after miRNA transfection into phGFs.

For each miRNA, the 10 most downregulated target genes with a miRNA target score ≥ 80 are listed. Previously reported periodontitis risk genes are highlighted in bold letters.

miRNA	Gene	P_{adj}	Fold change (down)	Target Score
<i>hsa-miR-130a-3p</i>	<i>ENPP5</i>	6.9E-12	5.81	96
	<i>CPEB1</i>	1.7E-21	2.81	100
	<i>BMT2</i>	5.4E-29	2.79	92
	<i>IMPDH1</i>	1.3E-33	2.26	94
	<i>MYBL1</i>	2.0E-27	2.26	99
	<i>RTCA</i>	6.4E-42	2.24	95
	<i>THOP1</i>	1.4E-22	2.13	86
	<i>NACC2</i>	1.2E-25	2.13	92
	<i>DICER1</i>	2.8E-35	2.08	91
	<i>GAREM1</i>	2.5E-05	2.08	93
<i>hsa-miR-142-3p</i>	<i>WASL</i>	7.1E-140	6.87	94
	<i>SLC49A4</i>	3.2E-37	3.89	96
	<i>CFL2</i>	3.4E-74	3.89	88
	<i>NR2F6</i>	6.4E-53	3.85	83
	<i>TSEN34</i>	2.8E-74	3.73	94
	<i>AKT1S1</i>	2.9E-107	3.62	86
	<i>LRRC32</i>	2.5E-15	3.12	88
	<i>RARG</i>	8.7E-103	3.10	81
	<i>INPP5A</i>	1.8E-42	3.08	86
	<i>MRFAP1</i>	2.4E-94	2.94	89
<i>hsa-miR-144-3p*</i>	<i>UBE2D1</i>	3.7E-4	5.03	100
	<i>NACC2</i>	4.9E-56	4.47	99
	<i>IMPA1</i>	2.9E-24	4.44	90
	<i>FBN2</i>	1.2E-46	4.28	99
	<i>MYEF2</i>	2.9E-16	3.07	99
	<i>ATP5MC2</i>	1.8E-35	3.03	95
	<i>GPR176</i>	3.0E-16	2.96	84
	<i>ARNTL2</i>	4.3E-16	2.93	83
	<i>FZD6</i>	1.3E-16	2.87	99
	<i>MAPK6</i>	2.3E-23	2.77	99

	<i>MMD</i>	3.7E-23	4.47	86
	<i>FAM3C</i>	1.5E-45	3.92	81
	<i>RRAGC</i>	1.2E-43	3.27	92
	<i>ATP6V1C1</i>	8.1E-36	3.10	95
<i>hsa-miR-144-5p</i>	<i>APBB1</i>	2.4E-32	2.58	91
	<i>RAB33A</i>	2.8E-4	2.58	94
	<i>TFG</i>	1.2E-42	2.57	93
	<i>DRAM2</i>	3.1E-19	2.55	83
	<i>REEP3</i>	7.4E-28	2.51	83
	<i>ZSCAN31</i>	4.7E-9	2.45	84
	<i>IDH1</i>	9.00E-35	2.20	90
	<i>SEC23A</i>	1.50E-33	1.82	95
	<i>LRRC17</i>	1.70E-08	1.74	99
	<i>RARG</i>	2.40E-43	1.73	99
<i>hsa-miR-30e-5p</i>	<i>GALNT7</i>	5.40E-27	1.71	98
	<i>ADAM19</i>	7.70E-35	1.69	96
	<i>AVEN</i>	2.30E-19	1.47	81
	<i>SKP2</i>	1.10E-24	1.45	91
	<i>SCML1</i>	1.30E-26	1.44	98
	<i>TMEM181</i>	3.40E-39	1.42	98
	<i>ENPP5</i>	1.90E-09	2.53	100
	<i>PDCD1LG2</i>	1.50E-52	2.41	99
	<i>CYBRD1</i>	1.50E-47	2.37	89
	<i>TGFBR2</i>	4.10E-76	1.94	86
<i>hsa-miR-17-5p</i>	<i>FYCO1</i>	1.60E-36	1.87	100
	<i>LIMK1</i>	2.50E-42	1.83	94
	<i>KCNB1</i>	3.7E-04	1.65	99
	<i>ZNFX1</i>	1.90E-30	1.63	100
	<i>SLC40A1</i>	4.90E-14	1.58	99
	<i>TMEM64</i>	1.10E-22	1.53	89
<i>hsa-miR-223-3p</i>	<i>PARP1</i>	7.10E-56	1.64	89
	<i>TBC1D17</i>	1.70E-13	1.30	85
	<i>SLC35G2</i>	7.80E-17	1.28	93

<i>SLC7A8</i>	1.30E-16	1.26	91
<i>SLC4A4</i>	9.30E-18	1.24	97
<i>CBX5</i>	1.30E-17	1.18	95
<i>FBXO8</i>	6.40E-14	1.17	94
<i>ARMCX1</i>	7.40E-19	1.16	94
<i>RCN2</i>	1.00E-07	1.02	80

*Note that miRNA-144-3p regulates periodontitis risk gene *ABCA1* (FC downregulation = 2.23, $P_{adj} = 1.4 \times 10^{-19}$), which is on position 29.

3.2 Validation of the inhibitory effect of hsa-miR-130a-3p on the 3'UTR sequence of *CPEB1*.

After confirming the absence of genomic DNA contamination in the cDNA, qRT-PCR was conducted to validate that hsa-miR-130a-3p binds at the 3'_UTR of the gene *CPEB1*, cloned into the 3'_UTR of the *Luc* reporter gene, and that it downregulates *Luc* mRNA. To this end, a qRT-PCR was performed with *GAPDH* primers and *Luciferase* primers. 24 hours after miRNA transfection, the mRNA expression of *Luc* exhibited a downregulation of fold change of 2.56 in iHGF cells with a significance of $P = 0.0076$, as demonstrated in **Figure 8**.

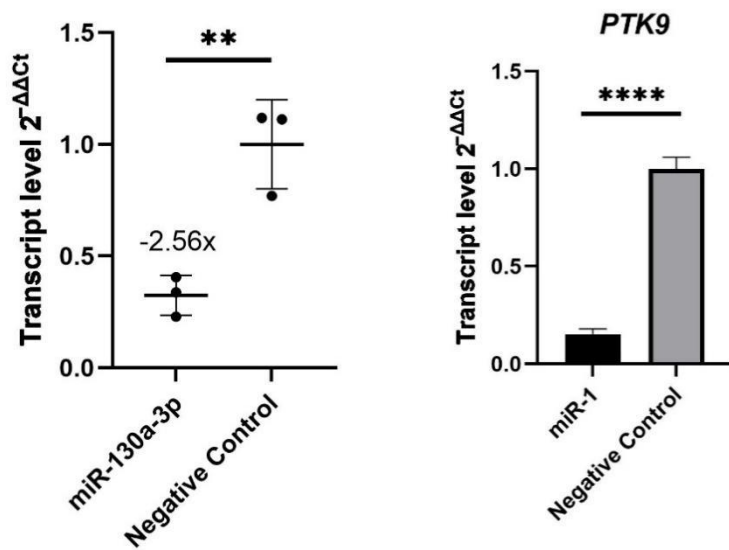


Figure 8. miR-130a-3p downregulates *CPEB1*-3'UTR *Luc* reporter gene expression in iHGFs.

(Left) Co-transfection of *CPEB1*-3'UTR *Luc* reporter gene plasmid and miR-130a-3p mimic significantly reduced *Luc* gene expression, with $P = 0.0076$, FC = -2.56. (Right) Co-transfection of *CPEB1*-3'UTR *Luc* reporter gene plasmid and miR-1 positive control mimics significantly reduced *PTK9* gene expression, with $P < 0.0001$.

3.3 Validation of the effect of hsa-miR-130a-3p on protein expression through dual luciferase reporter gene assay

To determine the effect of hsa-miR-130a-3p on the *CPEB1* 3'UTR binding site on the protein level, luciferase activity of the reporter gene was measured in iHGF cells 48 hours after co-transfection with Plasmid DNA and miRNA mimics. Luciferase activity was downregulated with a -2.0-fold change and a p-value of 0.0001 (**Figure 9**).

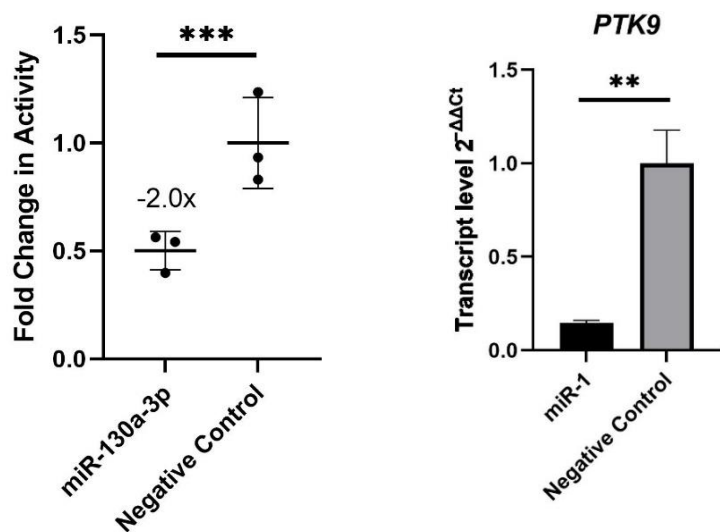


Figure 9. miR-130a-3p downregulates *CPEB1*-3'UTR *Luc* protein activity in iHGFs.

(Left) Co-transfection of *CPEB1*-3'UTR-*Luc* reporter gene plasmid with miR-130a-3p mimic significantly reduced *Luc* protein activity ($P = 0.0001$, FC=-2.0; chemiluminescence detection); (Right) Co-transfection of *CPEB1*-3'UTR *Luc* reporter gene plasmid and miR-1 positive control mimics significantly reduced *PTK9* gene expression, with $P = 0.0053$.

3.4 All miRNAs significantly upregulated the gene *MET*

miRNAs generally repress their target genes, but we found numerous upregulated genes after miRNA transfection. I noted that increased levels of each of the 7 selected miRNAs correlated with increased expression of the gene *MET* Proto-Oncogene, Receptor Tyrosine Kinase (*MET*) (**Figure 10, Table 19**).

The 3'UTR of *MET* mRNA contains no miRNA binding site for 5 miRNAs (has-miR-144-5p, -miR-142-3p, -miR-223-3p, -miR-17-5p, -miR-30e-5p). has-miR-144-3p had a very poorly conserved predicted *MET* binding site (target score 57) and has-miR-130a-3p had a more conserved *MET* binding site (target score 93). This indicated indirect regulation by most miRNAs, occurring upstream of *MET* expression in the different signaling cascades, which would converge downstream to increased *MET* expression, as observed in our experiments.

To add evidence to the observation that all miRNAs had effects on *MET* expression, we validated the RNA-Seq data on both the transcript and protein level. Separate transfection of each of the miRNA mimics for 24 hours resulted in a significant increase of *MET* mRNA transcript levels

(Figure 10A, Table 19). Additionally, we validated the observed increased expression of the genes *DDX3Y*, *RBPJ*, and *SLC36A1* by qRT-PCR (Figure 10A-D, Table 19).

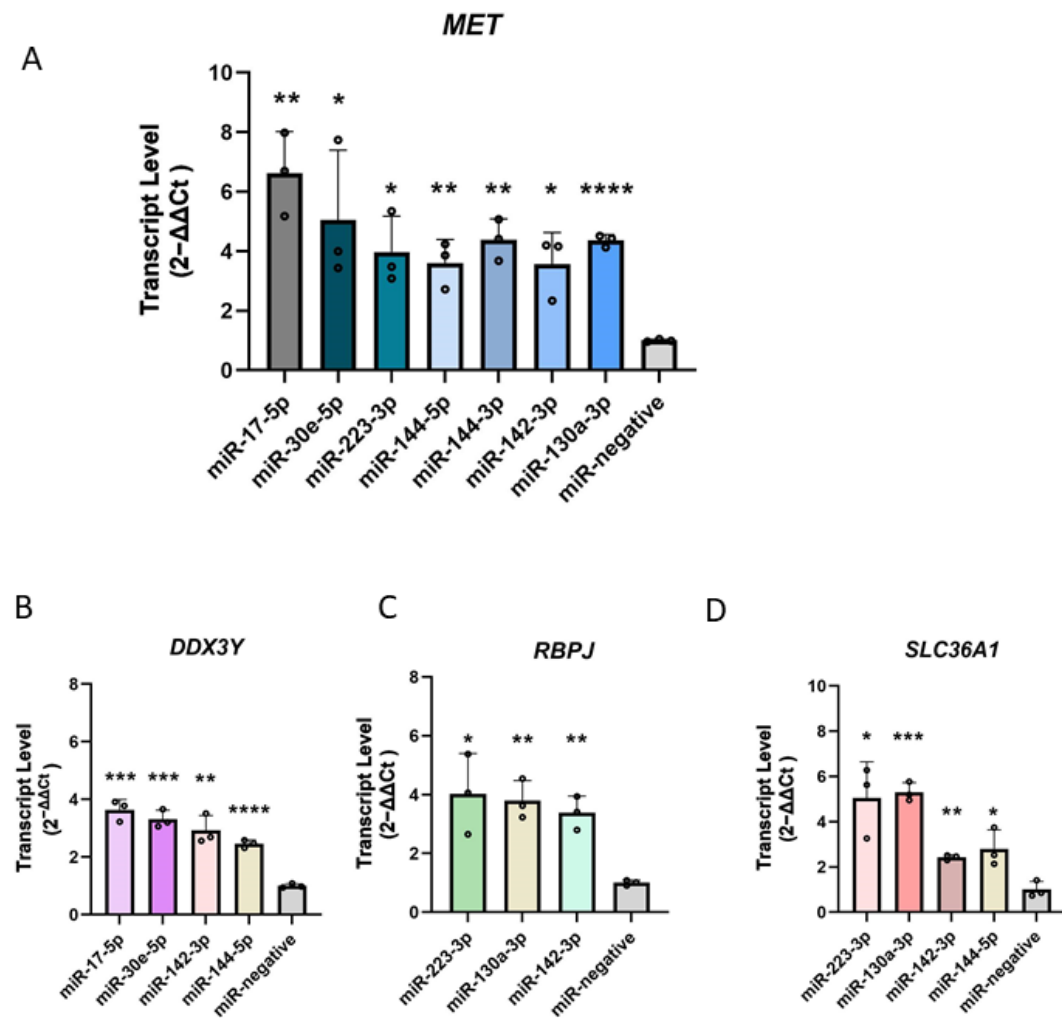


Figure 10. Transcript levels of *MET*, *RBPJ*, *DDX3Y* and *SLC36A1* after miRNA transfection in pHGFs.

Transfection of miRNA mimics significantly upregulated *MET* (A), *DDX3Y* (B), *RBPJ* (C), and *SLC36A1* (D) expression. *MET* was upregulated after transfection with miR-17-5p ($P = 0.0023$, FC = 6.61), miR-30e-5p ($P = 0.0397$, FC=5.05), miR-223-3p ($P = 0.0131$, FC=3.96), miR-144-5p ($P = 0.0046$, FC=3.60), miR-144-3p ($P = 0.0011$, FC=4.38), miR-142-3p ($P = 0.0141$, FC=3.56), and miR-130a-3p ($P < 0.0001$, FC=4.35); *RBPJ* was upregulated after transfection with miR-223-3p ($P = 0.0184$, FC = 4.03), miR-142-3p ($P=0.0020$, FC=3.38), and miR-130a-3p ($P = 0.0020$, FC=3.80); *SLC36A1* was upregulated after transfection with miR-144-5p ($P = 0.0266$, FC = 2.80), miR-130a-3p ($P = 0.00020$, FC=5.31), and miR-142-3p ($P = 0.0028$, FC=2.43); *DDX3Y* was upregulated after transfection with miR-30e-5p ($P = 0.0002$, FC=3.30), miR-144-5p ($P < 0.0001$, FC=2.45), miR-142-3p ($P = 0.0030$, FC=2.92), and miR-17-5p ($P = 0.0002$, FC = 3.63).

Table 19: Genes that were upregulated by ≥ 3 miRNAs

miRNA	Gene	RNA-seq	qRT-PCR

			logFC	P_{adj}	FC	P
hsa-miR-223-3p	<i>MET</i>	2.0	8.8 x 10 ⁻⁵⁶	3.9	0.0131	
	<i>SLC36A1</i>	1.5	1.5 x 10 ⁻³⁷	5.1	0.0126	
	<i>RBPJ</i>	1.3	8.7 x 10 ⁻²²	4.0	0.0184	
hsa-miR-30e-5p	<i>MET</i>	2.1	4.0 x 10 ⁻⁶¹	5.1	0.0397	
	<i>DDX3Y</i>	1.5	5.9 x 10 ⁻³⁰	3.3	2.0 x 10 ⁻⁴	
hsa-miR-17-5p	<i>MET</i>	1.9	3.9 x 10 ⁻⁴⁹	6.6	0.0023	
	<i>DDX3Y</i>	1.3	1.1 x 10 ⁻²²	3.6	2.0 x 10 ⁻⁴	
	<i>MET</i>	1.4	1.2 x 10 ⁻¹⁹	3.6	0.0046	
hsa-miR-144-5p	<i>DDX3Y</i>	1.4	5.3 x 10 ⁻²⁸	2.5	< 1.0 x 10 ⁻⁴	
	<i>SLC36A1</i>	1.7	9.8 x 10 ⁻³⁹	2.8	2.6 x 10 ⁻²	
hsa-miR-144-3p	<i>MET</i>	1.6	1.3 x 10 ⁻²³	4.4	0.0011	
	<i>MET</i>	1.7	1.5 x 10 ⁻⁷⁴	3.6	0.0141	
	<i>RBPJ</i>	1.5	1.8 x 10 ⁻⁶⁶	3.4	0.002	
hsa-miR-142-3p	<i>DDX3Y</i>	1.3	6.1 x 10 ⁻⁵³	2.9	0.003	
	<i>SLC36A1</i>	1.3	1.5 x 10 ⁻³⁹	2.43	0.0028	
	<i>MET</i>	1.1	4.8 x 10 ⁻³⁴	4.4	< 1.0 x 10 ⁻⁴	
hsa-miR-130a-3p	<i>RBPJ</i>	1.5	7.6 x 10 ⁻⁶⁸	5.31	0.0002	
	<i>SLC36A1</i>	1.4	1.8 x 10 ⁻⁴⁴	5.3	2.0 x 10 ⁻⁴	

3.5 Validation of the upregulation effect of hsa-miR-17-5p, -30e-5p, -223-3p, -142-3p, -130a-3p, -144-3p, -144-5p on the gene *MET* via Western blotting.

To provide evidence that *MET* was also upregulated on the protein level after miRNA transfection, Western blotting was performed following miRNA transfection.

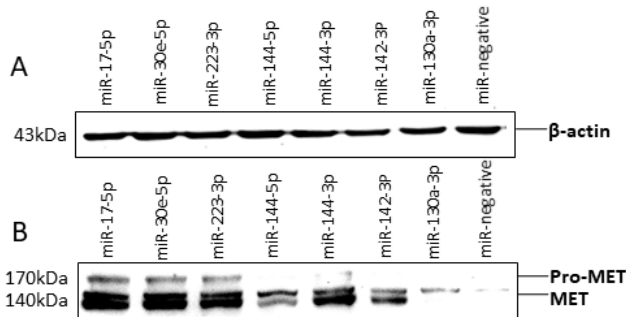


Figure 11. Western blot showed that transfection of each miRNA increased protein levels of *MET* in ihGFs.

A. β -actin(43kDa), B. MET(pro-MET: 170kDa, MET: 140kDa)

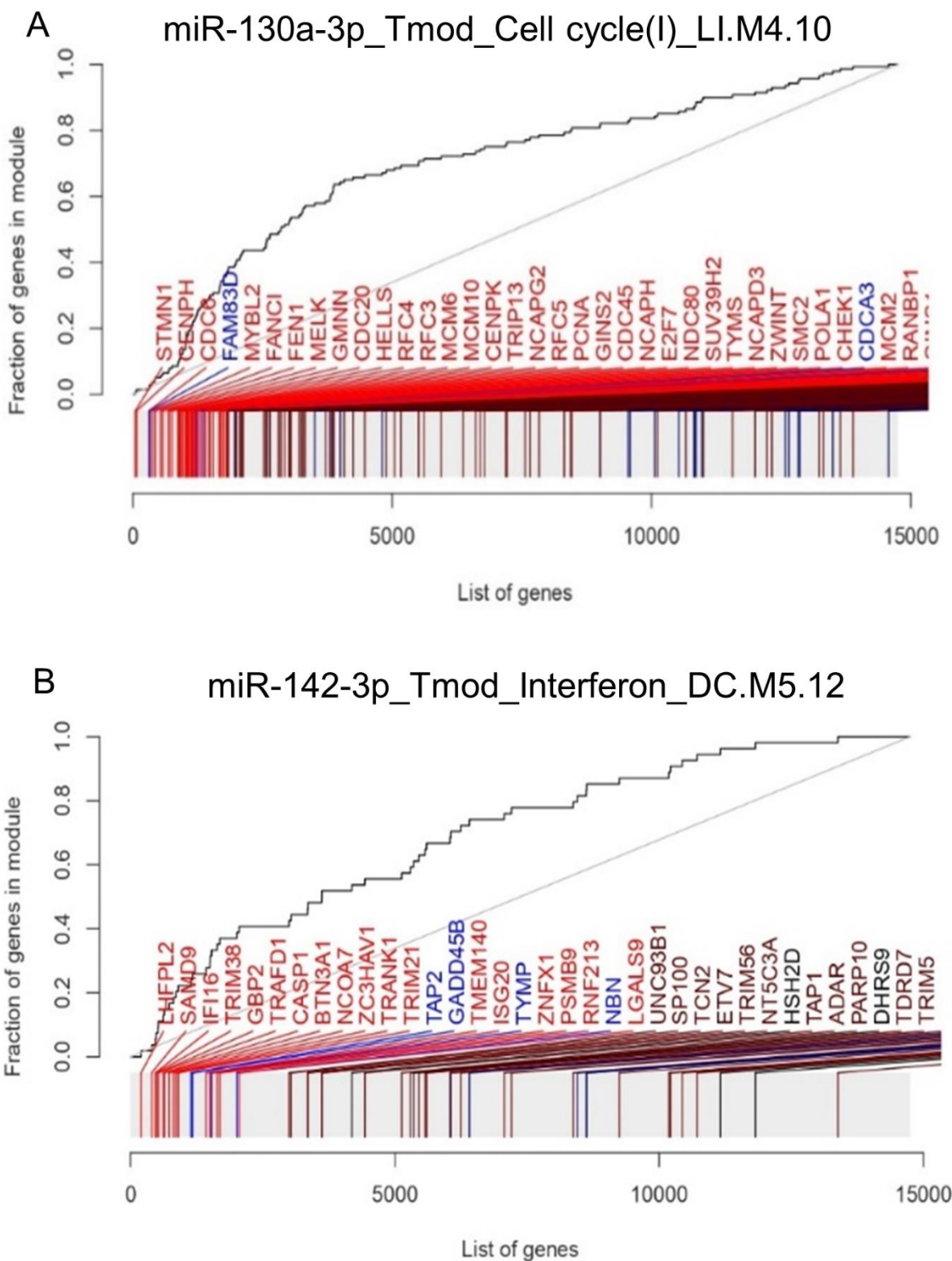
3.6 Gene set enrichment analyses

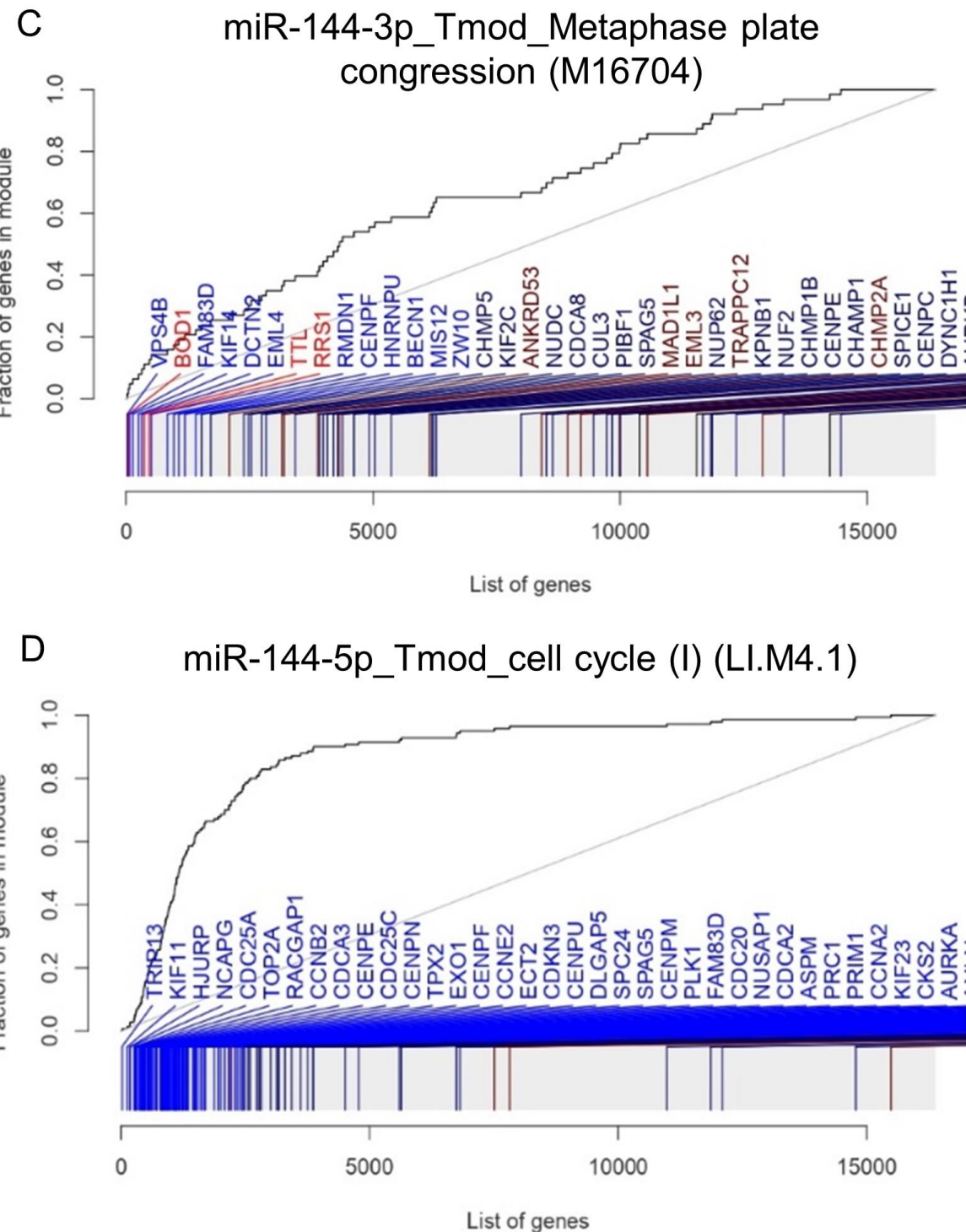
We subsequently performed a gene set enrichment analysis (GSEA) to identify miRNA regulated gene sets. At first, we tested enrichment of the specific MIR gene set. MIR130A_3P (ID: M30650) was enriched with $P = 9.5 \times 10^{-69}$ (AUC = 0.73), MIR142_3P (M31116) showed $P = 2.2 \times 10^{-98}$ (AUC = 0.89), MIR144-3p showed $P = 9 \times 10^{-106}$ (AUC = 0.74), MIR144-5p showed $P = 3.2 \times 10^{-31}$ (AUC = 0.9), MIR17-5p (ID:M30516) showed $P = 6.2 \times 10^{-127}$ (AUC = 0.74), MIR223-3p (ID:M31334) showed $P = 4.2 \times 10^{-27}$ (AUC = 0.73), MIR30e-5p (ID:M30442) showed $P = 1.6 \times 10^{-103}$ (AUC = 0.70). The enrichment of the miRNA genes sets specific to each miRNA proved the biologically functional effects of the transfected miRNA mimic, implying additional validity of our findings.

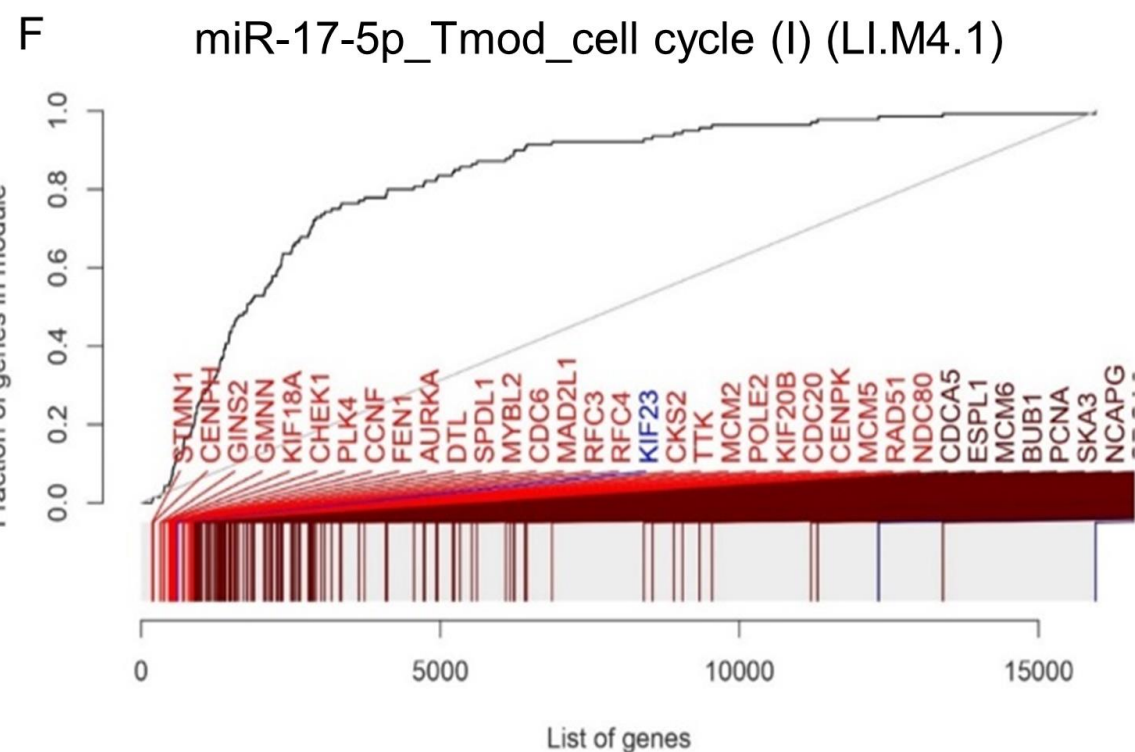
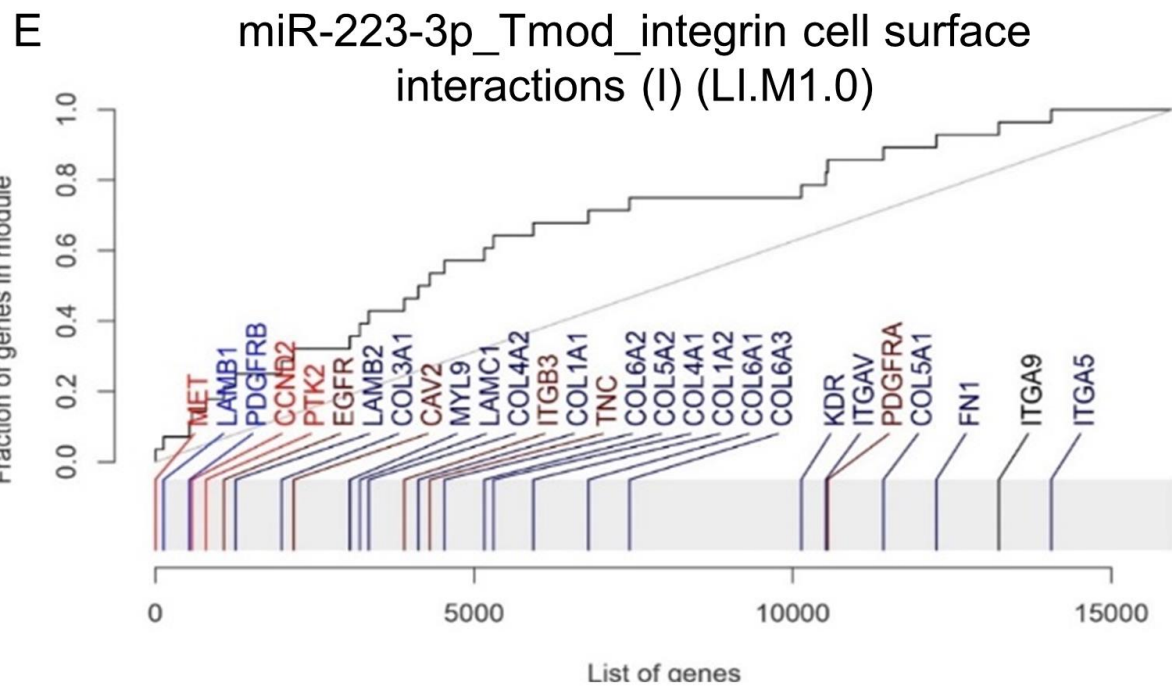
Next, we performed GSEA with the co-expression gene set tmmod and the Molecular Signatures Database (MSigDB) gene sets reactome, hallmark, KEGG and GO. The most significantly enriched gene sets found in the different collections are given in **Table 20 and Figure 12**.

For hsa-miR-130a-3p, the gene set collections indicated the most significant enrichment of gene sets involved in cell cycle regulation and cytokine signaling. For hsa-miR-142-3p, the gene set collections indicated regulation of cytokine signaling and cell locomotion including adherens junctions. For hsa-miRNA-144-3p, the gene set collections indicated the most significant enrichment of gene sets involved in extracellular matrix genes (tmmod) and regulation of cell division (GO) or Melanoma (Kegg). In addition, GO also indicated a more specific involvement in Platelet derived growth factor receptor signaling pathway and Regulation of vascular associated smooth muscle cell proliferation and others. For miRNA-144-5p, all gene set collections unanimously indicated functionality in mitotic cell cycle. For hsa-miR-17-5p and hsa-miR-30e-5p, the gene set collections indicated the most significant enrichment of gene sets involved in cell cycle regulation and

transcription. For hsa-miR-223-3p, the gene set collections indicated regulation of integrin cell surface interactions.







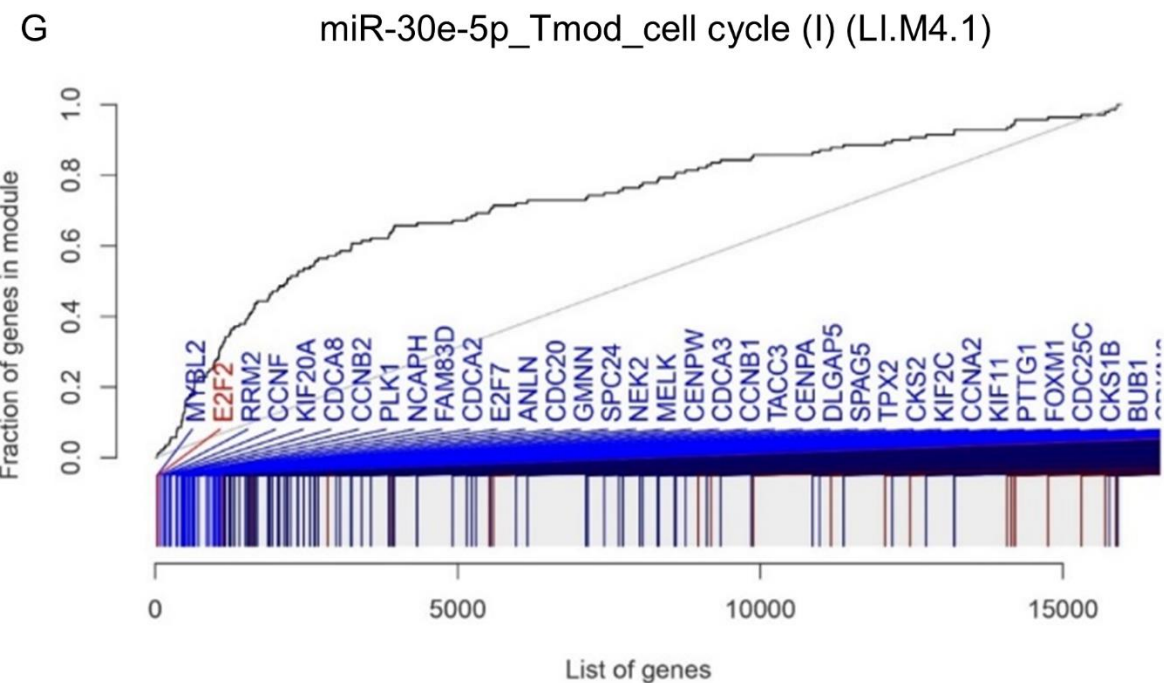


Figure 12. Evidence plots of enriched gene sets indicated cell cycle and innate immunity pathways as being regulated by each of the miRNAs. The most significant enriched gene set of each of the analysed gene set collections for each miRNA is shown.

Table 20: The most significantly enriched gene set for each gene set collection after miRNA transfection into phGFs.

miRNA	Gene set	ID	Collection	genes	AUC	Padj
hsa-miR -130a-3p	TNFA signaling via NFKB	M5890	Hallmark	190	0.66	5.0 x 10 ⁻¹⁵
	Cell cycle	M14460	GO	1,598	0.58	5.7 x 10 ⁻¹⁵
	Cell cycle (I)	LI.M4.1	Tmod	140	0.70	9.6 x 10 ⁻⁹
	Cytokine signaling in immune system	M1060	Reactome	660	0.58	8.0 x 10 ⁻⁸
	Pathways in cancer	M12868	KEGG	271	0.59	5.3 x 10 ⁻⁵
hsa-miR -142-3p	Locomotion	M13680	GO	1370	0.56	1.1 x 10 ⁻¹¹
	TNFA signaling via NFKB	M5890	Hallmark	190	0.65	4.7 x 10 ⁻¹¹
	Cytokine signaling in immune system	M1060	Reactome	660	0.57	1.1 x 10 ⁻⁷
	Adherens Junction	M638	KEGG	67	0.64	1.0 x 10 ⁻⁵
	Interferon	DC.M5.12	Tmod	54	0.69	1.3 x 10 ⁻²
hsa-miR -144-3p	Melanoma	M15798	KEGG	54	0.72	3.7x 10 ⁻⁶
	Metaphase plate congression	M16704	GO	63	0.66	1.5 x 10 ⁻⁴
	Extracellular matrix (I)	LI.M2.0	Tmod	30	0.77	2.0x 10 ⁻³
hsa-miR -144-5p	Cell cycle (I)	LI.M4.1	Tmod	140	0.88	3.0x 10 ⁻³⁷
	G2M checkpoint	M5901	Hallmark	199	0.72	4.8x 10 ⁻²³
	Mitotic prometaphase	M4217	Reactome	194	0.70	4.6x 10 ⁻¹⁵

	Sister chromatid segregation	M536	GO	186	0.65	2.5×10^{-10}
	Cell cycle	M7963	KEGG	122	0.65	2.3×10^{-5}
	Cell cycle (I)	LI.M4.1	Tmod	140	0.83	9.5×10^{-23}
	REACTOME_RESOLUTION_OF_SISTER_CHROMATID_COHESION	M27181	Reactome	117	0.67	4.2×10^{-6}
hsa-miR-17-5p	E2F_TARGETS	M5925	Hallmark	200	0.72	8.3×10^{-16}
	REPLICATION	M16853	Kegg	36	0.74	5.8×10^{-4}
	GOBP_NEGATIVE_REGULATION_OF_SMALL_GTPASE_MEDIATED_SIGNAL_TRANSDUCTION	M11863	Go	50	0.66	8.8×10^{-6}
	integrin cell surface interactions (I)	LI.M1.0	Tmod	28	0.67	3.2×10^{-2}
	REACTOME_MET_PROMOTES_CELL_MOTILITY	M27778	Reactome	39	0.72	1.6×10^{-4}
hsa-miR-223-3p	KEGG_RENAL_CELL_CARCINOMA	M13266	Kegg	64	0.68	4.8×10^{-5}
	GOBP_REGULATION_OF_PROTEIN_LOCALIZATION_TO_NUCLEUS	M15292	Go	115	0.65	6.9×10^{-5}
	Cell cycle (I)	LI.M4.1	Tmod	140	0.73	8.2×10^{-18}
	REACTOME_REGULATION_OF_CHOLESTEROL BIOSYNTHESIS_BY_SREBP_SREBF	M27001	Reactome	55	0.66	2.7×10^{-3}
hsa-miR-30e-5p	HALLMARK_G2M_CHECKPOINT	M5901	Hallmark	198	0.66	2.8×10^{-12}
	GOBP_ATTACHMENT_OF_SPINDLE_MICROTUBULES_TO_KINETOCHOR	M10211	Go	35	0.73	2.7×10^{-3}

4. Discussion

In the current study, we identified the target genes and gene sets regulated by 7 miRNAs upregulated in periodontitis. We found that 3 miRNAs regulated a periodontitis risk gene. These were *CPEB1* (Rhodin et al. 2014), *ABCA1* (Richter et al. 2022; Teumer et al. 2013), and *ATP6V1C1* (Munz et al. 2019), which were regulated by hsa-miR-130a-3p, hsa-miR-144-3p and hsa-miR-144-5p, respectively. Moreover, these genes were among the 10 most downregulated genes following miRNA upregulation. It had been reported before that these miRNAs regulate *ABCA1* and *ATP6V1C1* (Capstone Project: Data Science DSC180B; Genetic Overlap between Alzheimer's, Parkinson's, and healthy patients; replication project for the papers (Burgos et al. 2014; de Aguiar Vallim et al. 2013; Wu et al. 2019). Our data validated the regulation in ihGFs and showed its significance for oral inflammation. Regulation of *CPEB1* by hsa-miR-130a-3p has not been reported before. We validated this interaction by showing that the specific hsa-miR-130a-3p binding sites within the 3'UTR of *CPEB1* were sufficient to repress transcript levels and protein activity of a reporter gene. *CPEB1* encodes a member of the cytoplasmic polyadenylation element binding protein family. This highly conserved protein binds to a specific RNA consensus sequence (5'-UUUUUAU-3') found in the 3'-UTR of some mRNAs, and directs cytoplasmic polyadenylation as well as mediating both translational activation and repression (Mendez and Richter 2001; Welk et al. 2001). *CPEB1*, as well as *CPEB4*, encoded by another risk gene of periodontitis (Freitag-Wolf et al. 2021), is essential for successful mitotic cell division and has sequential non-redundant functions which promote the phase-specific polyadenylation and translational activation of CPE-regulated transcripts in the mitotic cell cycle. In particular, *CPEB1* is specifically required for prophase entry and *CPEB4* for cytokinesis (Giangarra et al. 2015).

ABCA1, *ATP6V1C1* and *CPEB1* are currently being considered as suggestive risk genes of periodontitis because their associations did not reach genomewide significance ($p < 5 \times 10^{-8}$) in the explorative GWAS'. We consider that the independent discovery of these genes as targets for miRNA, which are upregulated in inflamed gingiva, adds evidence to their status as susceptibility genes of periodontitis.

After overexpression of hsa-miR-142-3p, the gene *WASL* showed the most significant and strongest downregulation of this miRNA's target genes. A recent study showed that *WASL* deficiency in hGFs activated the signaling pathways of NF- κ B and MAPK, thereby increasing the production and infiltration of inflammatory cytokines and proliferation of keratinocytes (Kalailingam et al. 2017; Wang et al. 2020). *WASL* is involved in actin cytoskeletal reorganization including signal-

dependent regulation of actin dynamics, which is, for example, essential for cell locomotion (Stradal et al. 2004). Correspondingly, we found that the most hsa-miR-142-3p enriched gene sets were TNFA_SIGNALING_VIA_NFKB (Hallmark), GO_LOCOMOTION and GO_CYTOSKELETON_ORGANIZATION (GO).

For the other miRNAs, GSEA also indicated specific biological functions. hsa-miR-130a-3p transfection enriched the gene sets CELL CYCLE (tmmod, GO) and CYTOKINE SIGNALING (KEGG, Hallmark, Reactome). The two hsa-miR-144 transcripts have a role in the regulation of cell proliferation. hsa-miR-144-3p showed the strongest enrichment of the gene sets MELANOMA (KEGG) and cell division (METAPHASE PLATE CONGRESSION; GO), corresponding with recent findings of a role in the regulation of cell proliferation in various cancers (Sun et al. 2020). hsa-miR-144-5p also regulates the cell cycle, unanimously shown by all gene set collections in the GSEA. Further reliability of our data was added by the recovery of 3 known target genes of hsa-miR-144-3p within the top 10 of its most downregulated genes. These were the periodontitis risk gene *ABCA1* (de Aguiar Vallim et al. 2013), *FBN2* (fibrillin 2) (Mo et al. 2021) and *MAPK6* (mitogen-activated protein kinase 6) (Wu et al. 2019). *FBN2* is a component of connective tissue microfibrils. It is supposed to regulate osteoblast maturation by controlling TGF-beta bioavailability (inferred from sequence similarity, Uniprot). The function of *MAPK6* is unclear, but it may promote entry in the cell cycle (by similarity, Uniprot). In mice, knockdown of the *ATP6V1C1* orthologue severely impaired osteoclast acidification activity and bone resorption (Feng et al. 2009).

As the AUC values were often < 0.8 , this limited the significance of the GSEA. We consider more subtle regulatory effects of miRNAs compared to transcription factors (TFs) caused these moderate effects. Although miRNAs like TFs can exert a widespread impact on gene expression, hierarchically, miRNAs function downstream of TFs since miRNAs can repress an mRNA only after it has already been transcribed. Additionally, whereas TFs abundantly bind in the genome and can regulate several hundreds to over a thousand genes (Goolam et al. 2020; Lopez-Pajares et al. 2015), miRNAs repress an average 200 transcripts (Lewis et al. 2005), which also corresponds to our results.

miRNAs typically inhibit gene activity. However, despite lacking conserved binding sites for the studied miRNAs, we observed upregulation or altered expression of certain genes following miRNA transfection. This suggests that the repression of inhibitory genes may result in reduced repression of downstream signaling cascade genes. Notably, each miRNA significantly increased the expression of the *MET* gene. This implies that the selected gingival inflammatory miRNAs all converge different signaling networks to *MET* expression. This argues for a relevant role of

MET in the disease etiology, particularly during the stage when the gingival tissue biopsies were collected. To prove this finding, I validated the RNA-Seq data by qRT-PCR as an alternative technical method. Additionally, I re-transfected each miRNA separately and performed protein blotting, which proved there was increased *MET* expression after miRNA transfection on the protein level. *MET* was described as the cell-surface receptor for hepatocyte growth factor (HGF) (Bottaro et al. 1991). HGF, secreted by fibroblasts, exhibits angiogenic and mitogenic effects on epithelial and endothelial cells. *MET* may play a role in the transition from active inflammation to tissue regeneration, which coincides with the timing of tissue sampling before periodontal surgery, typically performed after active inflammation subsides. During this transition, granulation tissue forms, characterized by proliferating fibroblasts, extracellular matrix remodeling, and sprouting angiogenesis. GSEA results indicated that the selected miRNAs regulate these processes.

In conclusion, this study identified miRNAs that are upregulated in periodontitis and directly target various periodontitis risk genes. It suggests a significant role for *MET* in the transition from active inflammation to tissue regeneration. However, further investigation is required to explore the direct regulatory pathways upstream of the *MET* gene as well as its downstream regulatory pathways, which is also a limitation of this study. Profiling miRNA expression in gingival tissues at different disease stages could uncover additional core genes specific to each stage of periodontitis and gingival healing, offering potential therapeutic targets.

5. Conclusion

This thesis showed the target genes and gene sets of the 7 miRNAs that were upregulated in periodontal inflammation. These miRNAs regulate cytokine signaling, cell cycle and division and downregulate the periodontitis risk genes *CPEB1*, *ABCA1* and *ATP6V1C1*. Additionally, all of the selected miRNAs significantly upregulated the gene MET Proto-Oncogene, Receptor Tyrosine Kinase (*MET*). This indicated indirect regulation by most miRNAs, occurring upstream in the different signaling cascades, which would converge downstream to increased *MET* expression, as observed in my experiments. This argues for a relevant role of *MET* in the disease etiology, particularly during the stage when the gingival tissue biopsies were collected. To prove this finding, I validated the RNA-Seq data by qRT-PCR as an alternative technical method. Additionally, I re-transfected each miRNA separately and performed protein blotting, which proved increased *MET* expression after miRNA transfection on the protein level.

Moreover, within this thesis, miRNA hsa-miR-130a-3p was identified as a transcriptional repressor of the gene *CPEB1*, an essential component for successful mitotic cell division. *CPEB1*, along with *CPEB4*, encoded by another periodontitis risk gene, plays a crucial role in the phase-specific polyadenylation and translational activation of CPE-regulated transcripts during the mitotic cell cycle. This thesis provided mechanistic evidence demonstrating that increased expression of hsa-miR-130a-3p leads to reduced transcript levels and protein activity of a reporter gene expressing the *CPEB1* 3'UTR. The molecular mechanism underlying this effect was shown to be consistent across different cell types, as observed in Immortalized Human Gingival Fibroblasts and Primary Human Gingival Fibroblasts. In conclusion, these experiments revealed that hsa-miR-130a-3p interacts with the 3' UTR of *CPEB1*, resulting in gene expression suppression through mRNA degradation.

However, to gain a comprehensive understanding of the regulatory mechanisms involving the *MET* gene, it is imperative to conduct additional investigations that delve into both its upstream and downstream regulatory pathways. This aspect represents a notable limitation of the present study, as the direct regulatory pathways preceding the gene *MET*, as well as the subsequent pathways it influences, require further exploration. By addressing this limitation, future research endeavors can unravel the intricate network of regulatory factors governing the gene *MET* and provide a more comprehensive picture of its functional implications.

References

- Altun E, Walther C, Borof K, Petersen E, Lieske B, Kasapoudis D, Jalilvand N, Beikler T, Jagemann B, Zyriax BC et al. 2021. Association between dietary pattern and periodontitis-a cross-sectional study. *Nutrients.* 13(11).
- Bakdash B. 1994. Oral hygiene and compliance as risk-factors in periodontitis. *J Periodontol.* 65(5):539-544.
- Bottaro DP, Rubin JS, Faletto DL, Chan AM, Kmiecik TE, Vande Woude GF, Aaronson SA. 1991. Identification of the hepatocyte growth factor receptor as the c-met proto-oncogene product. *Science.* 251(4995):802-804.
- Brennecke J, Stark A, Russell RB, Cohen SM. 2005. Principles of microRNA-target recognition. *PLoS Biol.* 3(3):e85.
- Burgos K, Malenica I, Metpally R, Courtright A, Rakela B, Beach T, Shill H, Adler C, Sabbagh M, Villa S et al. 2014. Profiles of extracellular mirna in cerebrospinal fluid and serum from patients with alzheimer's and parkinson's diseases correlate with disease status and features of pathology. *PLoS One.* 9(5):e94839.
- Chen Y, Wang X. 2020. Mirdb: An online database for prediction of functional microRNA targets. *Nucleic Acids Res.* 48(D1):D127-D131.
- Chopra A, Mueller R, Weiner J, 3rd, Rosowski J, Dommisch H, Grohmann E, Schaefer AS. 2022. Bach1 binding links the genetic risk for severe periodontitis with st8sia1. *J Dent Res.* 101(1):93-101.
- de Aguiar Vallim TQ, Tarling EJ, Kim T, Civelek M, Baldan A, Esau C, Edwards PA. 2013. MicroRNA-144 regulates hepatic atp binding cassette transporter a1 and plasma high-density lipoprotein after activation of the nuclear receptor farnesoid x receptor. *Circulation research.* 112(12):1602-1612.
- DeLuca DS, Levin JZ, Sivachenko A, Fennell T, Nazaire MD, Williams C, Reich M, Winckler W, Getz G. 2012. Rna-seqc: Rna-seq metrics for quality control and process optimization. *Bioinformatics.* 28(11):1530-1532.
- Dobin A, Davis CA, Schlesinger F, Drenkow J, Zaleski C, Jha S, Batut P, Chaisson M, Gingeras TR. 2013. Star: Ultrafast universal rna-seq aligner. *Bioinformatics.* 29(1):15-21.
- Eke PI, Dye BA, Wei L, Thornton-Evans GO, Genco RJ, Cdc Periodontal Disease Surveillance workgroup: James Beck GDRP. 2012. Prevalence of periodontitis in adults in the united states: 2009 and 2010. *J Dent Res.* 91(10):914-920.
- Ewels P, Krueger F, Kaller M, Andrews S. 2016. Cluster flow: A user-friendly bioinformatics workflow tool. *F1000Res.* 5:2824.
- Feng S, Deng L, Chen W, Shao J, Xu G, Li YP. 2009. At6v1c1 is an essential component of the osteoclast proton pump and in f-actin ring formation in osteoclasts. *Biochem J.* 417(1):195-203.
- Freitag-Wolf S, Munz M, Junge O, Graetz C, Jockel-Schneider Y, Staufenbiel I, Bruckmann C, Lieb W, Franke A, Loos BG et al. 2021. Sex-specific genetic factors affect the risk of early-onset periodontitis in europeans. *J Clin Periodontol.* 48(11):1404-1413.
- Fujimori K, Yoneda T, Tomofuji T, Ekuni D, Azuma T, Maruyama T, Mizuno H, Sugiura Y, Morita M. 2019. Detection of salivary miRNAs reflecting chronic periodontitis: A pilot study. *Molecules.* 24(6).
- Giangarra V, Igea A, Castellazzi CL, Bava FA, Mendez R. 2015. Global analysis of cpebs reveals sequential and non-redundant functions in mitotic cell cycle. *PLoS One.* 10(9):e0138794.

- Goolam M, Xypolita ME, Costello I, Lydon JP, DeMayo FJ, Bikoff EK, Robertson EJ, Mould AW. 2020. The transcriptional repressor blimp1/prdm1 regulates the maternal decidua response in mice. *Nat Commun.* 11(1):2782.
- Ha M, Kim VN. 2014. Regulation of microRNA biogenesis. *Nature reviews Molecular cell biology.* 15(8):509-524.
- Hamdi Z, Detzen L, Fessi S, Julia C, Hercberg S, Czernichow S, Boillot A, Touvier M, Bouchard P, Andreeva VA et al. 2021. Alcoholic beverage consumption, smoking habits, and periodontitis: A cross-sectional investigation of the nutrinet-sante study. *J Periodontol.* 92(5):727-737.
- Heasman PA, Hughes FJ. 2014. Drugs, medications and periodontal disease. *Br Dent J.* 217(8):411-419.
- Kalailingam P, Tan HB, Jain N, Sng MK, Chan JSK, Tan NS, Thanabalu T. 2017. Conditional knock out of n-wasp in keratinocytes causes skin barrier defects and atopic dermatitis-like inflammation. *Sci Rep.* 7(1):7311.
- Lall S, Grun D, Krek A, Chen K, Wang YL, Dewey CN, Sood P, Colombo T, Bray N, Macmenamin P et al. 2006. A genome-wide map of conserved microRNA targets in *C. elegans*. *Curr Biol.* 16(5):460-471.
- Lang NP, Schatzle MA, Loe H. 2009. Gingivitis as a risk factor in periodontal disease. *Journal of Clinical Periodontology.* 36:3-8.
- Lee YH, Na HS, Jeong SY, Jeong SH, Park HR, Chung J. 2011. Comparison of inflammatory microRNA expression in healthy and periodontitis tissues. *Biocell.* 35(2):43-49.
- Lewis BP, Burge CB, Bartel DP. 2005. Conserved seed pairing, often flanked by adenines, indicates that thousands of human genes are microRNA targets. *Cell.* 120(1):15-20.
- Li Y, Wang L, Xu X, Sun H, Wu L. 2021. Lncrna hla complex group 11 knockdown alleviates cisplatin resistance in gastric cancer by targeting the mir-144-3p/ube2d1 axis. *Cancer management and research.* 13:7543-7557.
- Liberzon A, Birger C, Thorvaldsdottir H, Ghandi M, Mesirov JP, Tamayo P. 2015. The molecular signatures database (msigdb) hallmark gene set collection. *Cell Syst.* 1(6):417-425.
- Loos BG, John RP, Laine ML. 2005. Identification of genetic risk factors for periodontitis and possible mechanisms of action. *Journal of Clinical Periodontology.* 32:159-179.
- Lopez-Pajares V, Qu K, Zhang J, Webster DE, Barajas BC, Siprashvili Z, Zarnegar BJ, Boxer LD, Rios EJ, Tao S et al. 2015. A lncrna-maf:Marb transcription factor network regulates epidermal differentiation. *Dev Cell.* 32(6):693-706.
- Love MI, Huber W, Anders S. 2014. Moderated estimation of fold change and dispersion for RNA-seq data with *deseq2*. *Genome Biol.* 15(12):550.
- Mascarenhas P, Gapski R, Al-Shammari K, Wang HL. 2003. Influence of sex hormones on the periodontium. *Journal of Clinical Periodontology.* 30(8):671-681.
- Matthews JC, Hori K, Cormier MJ. 1977. Substrate and substrate analogue binding properties of renilla luciferase. *Biochemistry.* 16(24):5217-5220.
- Mendez R, Richter JD. 2001. Translational control by cpeb: A means to the end. *Nat Rev Mol Cell Biol.* 2(7):521-529.
- Meyle J, Chapple I. 2015. Molecular aspects of the pathogenesis of periodontitis. *Periodontol 2000.* 69(1):7-17.
- Mo BY, Pang JS, Dai WB, Su YS, Jiang W, Huang SN. 2021. A comprehensive evaluation of miR-144-3p expression and its targets in laryngeal squamous cell carcinoma. *Comput Math Methods Med.* 2021:6684186.
- Munz M, Richter GM, Loos BG, Jepsen S, Divaris K, Offenbacher S, Teumer A, Holtfreter B, Kocher T, Bruckmann C et al. 2019. Meta-analysis of genome-wide association studies of aggressive and chronic periodontitis identifies two novel risk loci. *Eur J Hum Genet.* 27(1):102-113.

- Nesse W, Abbas F, van der Ploeg I, Spijkervet FK, Dijkstra PU, Vissink A. 2008. Periodontal inflamed surface area: Quantifying inflammatory burden. *J Clin Periodontol.* 35(8):668-673.
- Nield H. 2021. Lindhe's clinical periodontology and implant dentistry (7th edition) [two volumes]. *Brit Dent J.* 231(10):613-613.
- Ogata Y, Matsui S, Kato A, Zhou L, Nakayama Y, Takai H. 2014. Microrna expression in inflamed and noninflamed gingival tissues from Japanese patients. *J Oral Sci.* 56(4):253-260.
- Paul P, Chakraborty A, Sarkar D, Langthasa M, Rahman M, Bari M, Singha RS, Malakar AK, Chakraborty S. 2018. Interplay between miRNAs and human diseases. *Journal of cellular physiology.* 233(3):2007-2018.
- Perri R, Nares S, Zhang S, Barros SP, Offenbacher S. 2012. MiRNA modulation in obesity and periodontitis. *J Dent Res.* 91(1):33-38.
- Preshaw PM, Bissett SM. 2019. Periodontitis and diabetes. *Brit Dent J.* 227(7):577-584.
- Rhodin K, Divaris K, North KE, Barros SP, Moss K, Beck JD, Offenbacher S. 2014. Chronic periodontitis genome-wide association studies: Gene-centric and gene set enrichment analyses. *J Dent Res.* 93(9):882-890.
- Richter GM, Kruppa J, Keceli HG, Ataman-Duruel ET, Graetz C, Pisched N, Wagner G, Rendenbach C, Jockel-Schneider Y, Martins O et al. 2021. Epigenetic adaptations of the masticatory mucosa to periodontal inflammation. *Clin Epigenetics.* 13(1):203.
- Richter GM, Wagner G, Reichenmiller K, Staufenbiel I, Martins O, Loscher BS, Holtgrewe M, Jepsen S, Dommisch H, Schaefer AS. 2022. Exome sequencing of 5 families with severe early-onset periodontitis. *J Dent Res.* 101(2):151-157.
- Sayols S, Scherzinger D, Klein H. 2016. Duprader: A bioconductor package for the assessment of PCR artifacts in RNA-seq data. *BMC Bioinformatics.* 17(1):428.
- Selbach M, Schwanhausser B, Thierfelder N, Fang Z, Khanin R, Rajewsky N. 2008. Widespread changes in protein synthesis induced by miRNAs. *Nature.* 455(7209):58-63.
- Stoecklin-Wasmer C, Guarnieri P, Celenti R, Demmer RT, Kebschull M, Papapanou PN. 2012. MiRNAs and their target genes in gingival tissues. *J Dent Res.* 91(10):934-940.
- Stradal TE, Rottner K, Disanza A, Confalonieri S, Innocenti M, Scita G. 2004. Regulation of actin dynamics by wasp and wave family proteins. *Trends Cell Biol.* 14(6):303-311.
- Sun N, Zhang L, Zhang C, Yuan Y. 2020. Mir-144-3p inhibits cell proliferation of colorectal cancer cells by targeting bcl6 via inhibition of wnt/beta-catenin signaling. *Cell Mol Biol Lett.* 25:19.
- Teumer A, Holtfreter B, Volker U, Petersmann A, Nauck M, Biffar R, Volzke H, Kroemer HK, Meisel P, Homuth G et al. 2013. Genome-wide association study of chronic periodontitis in a general German population. *J Clin Periodontol.* 40(11):977-985.
- Vos T, Flaxman AD, Naghavi M, Lozano R, Michaud C, Ezzati M, Shibuya K, Salomon JA, Abdalla S, Aboyans V et al. 2012. Years lived with disability (YLDs) for 1160 sequelae of 289 diseases and injuries 1990-2010: A systematic analysis for the global burden of disease study 2010. *Lancet.* 380(9859):2163-2196.
- Wang Y, Kang W, Shang L, Song A, Ge S. 2020. N-wasp knockdown upregulates inflammatory cytokines expression in human gingival fibroblasts. *Arch Oral Biol.* 110:104605.
- Welk JF, Charlesworth A, Smith GD, MacNicol AM. 2001. Identification and characterization of the gene encoding human cytoplasmic polyadenylation element binding protein. *Gene.* 263(1-2):113-120.
- Wu J, Zhao Y, Li F, Qiao B. 2019. Mir-144-3p: A novel tumor suppressor targeting mapk6 in cervical cancer. *J Physiol Biochem.* 75(2):143-152.
- Xie YF, Shu R, Jiang SY, Liu DL, Zhang XL. 2011. Comparison of miRNA profiles of human periodontal diseased and healthy gingival tissues. *Int J Oral Sci.* 3(3):125-134.

- Young MD, Wakefield MJ, Smyth GK, Oshlack A. 2010. Gene ontology analysis for rna-seq: Accounting for selection bias. *Genome Biol.* 11(2):R14.
- Zhao Y, Srivastava D. 2007. A developmental view of microrna function. *Trends Biochem Sci.* 32(4):189-197.
- Zyla J, Marczyk M, Domaszewska T, Kaufmann SHE, Polanska J, Weiner J. 2019. Gene set enrichment for reproducible science: Comparison of cerno and eight other algorithms. *Bioinformatics.* 35(24):5146-5154.

Statutory Declaration

"I, [Luyang, Zheng], by personally signing this document in lieu of an oath, hereby affirm that I prepared the submitted dissertation on the topic [Systematic search for microRNA regulated target genes with roles in the etiology of periodontitis / Systematische Suche nach mikroRNA-regulierten Zielgenen mit Rolle in der Ätiologie der Parodontitis], independently and without the support of third parties, and that I used no other sources and aids than those stated.

All parts which are based on the publications or presentations of other authors, either in letter or in spirit, are specified as such in accordance with the citing guidelines. The sections on methodology (in particular regarding practical work, laboratory regulations, statistical processing) and results (in particular regarding figures, charts and tables) are exclusively my responsibility.

Furthermore, I declare that I have correctly marked all of the data, the analyses, and the conclusions generated from data obtained in collaboration with other persons, and that I have correctly marked my own contribution and the contributions of other persons (cf. declaration of contribution). I have correctly marked all texts or parts of texts that were generated in collaboration with other persons.

My contributions to any publications to this dissertation correspond to those stated in the below joint declaration made together with the supervisor. All publications created within the scope of the dissertation comply with the guidelines of the ICMJE (International Committee of Medical Journal Editors; <http://www.icmje.org>) on authorship. In addition, I declare that I shall comply with the regulations of Charité – Universitätsmedizin Berlin on ensuring good scientific practice.

I declare that I have not yet submitted this dissertation in identical or similar form to another Faculty.

The significance of this statutory declaration and the consequences of a false statutory declaration under criminal law (Sections 156, 161 of the German Criminal Code) are known to me."

Date

Signature

Mein Lebenslauf wird aus datenschutzrechtlichen Gründen in der elektronischen Version meiner Arbeit nicht veröffentlicht.

Acknowledgements

I would like to seize this opportunity to express my appreciation to all those who have assisted and motivated me throughout my doctoral studies. The accomplishment of this work is owed to the contribution, aid, and backing of many supportive individuals.

First and foremost, I would like to express my sincere gratitude to Professor Arne Schäfer for giving me the opportunity to join this warm team and for leading me into the field of genetics. Without his patient guidance, support, and encouragement, this project would not have been successfully completed.

Secondly, I extend my gratitude to all members of the research group 'Genetics of Oral Inflammatory Diseases': Avneesh Chopra, Ricarda Müller, Xin Bao, Jia-Hui Song, and Weiwei Shi. Thank you for your assistance throughout my project and for providing me with valuable suggestions.

Finally, I would like to express my sincere appreciation to my family, boyfriend, and all my friends. Without your unwavering support and encouragement throughout these three years, I would not have been able to achieve what I have today.

Confirmation by a statistician

The statistical significance of the project's data and the analysis method were verified by the statistician from Institut für Biometrie und klinische Epidemiologie (iBikE), and the proof document is provided for reference.



CharitéCentrum für Human- und Gesundheitswissenschaften

Charité | Campus Charité Mitte | 10117 Berlin

Name, Vorname: Zheng, Luyang
Emailadresse: luyang.zheng@charite.de
Matrikelnummer: 227765
PromotionsbetreuerIn: Univ.-Prof. Dr. rer. nat. Arne Schäfer
Promotionsinstitution / Klinik: Berlin Institute of Health

Institut für Biometrie und klinische Epidemiologie (iBikE)

Direktor: Prof. Dr. Frank Konietzschke

Postanschrift:
 Charitéplatz 1 | 10117 Berlin
 Besucheranschrift:
 Reinhardtstr. 58 | 10117 Berlin



Tel. +49 (0)30 450 562 161
 frank.konietzschke@charite.de
<https://biometrie.charite.de/>

Bescheinigung

Hiermit bescheinige ich, dass Frau Zheng innerhalb der Service Unit Biometrie des Instituts für Biometrie und klinische Epidemiologie (iBikE) bei mir eine statistische Beratung zu einem Promotionsvorhaben wahrgenommen hat. Folgende Beratungstermine wurden wahrgenommen:

- Termin 1: 01.06.2023

Folgende wesentliche Ratschläge hinsichtlich einer sinnvollen Auswertung und Interpretation der Daten wurden während der Beratung erteilt:

- Aufgrund der kleinen Fallzahl (n=3 pro Gruppe) vorzugsweise den nicht-parametrischen Mann-Whitney Test benutzen.

Diese Bescheinigung garantiert nicht die richtige Umsetzung der in der Beratung gemachten Vorschläge, die korrekte Durchführung der empfohlenen statistischen Verfahren und die richtige Darstellung und Interpretation der Ergebnisse. Die Verantwortung hierfür obliegt allein dem Promovierenden. Das Institut für Biometrie und klinische Epidemiologie übernimmt hierfür keine Haftung.

Datum: 01.06.2023

Nilufar Akbari Digital unterschrieben von Nilufar Akbari
Datum: 2023.06.01 10:53:13 +02'00'

Unterschrift BeraterIn, Institutsstempel

CHARITÉ Name der Beraterin: Nilufar Akbari
 UNIVERSITÄTSMEDIZIN BERLIN
 Institut für Biometrie und
 Klinische Epidemiologie
 Campus Charité Mitte
 Charitéplatz 1 | D-10117 Berlin
 Silbermannstr. 58